AN INVESTIGATION OF PARTIAL DISCHARGE INCEPTION VOLTAGE IN AIR AND SF_6 GAS

A Thesis submitted
In partial fulfillment of the requirements
For the degree of

MASTER OF TECHNOLOGY

by

Partha Halder

to the

DEPARTMENT OF ELECTRICAL ENGINEERING
INDIAN INSTITUTE OF TECHNOLOGY KANPUR
DECEMBER 2000

CERTIFICATE

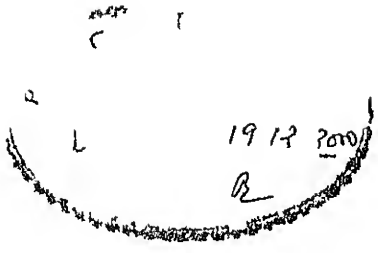

This work entitled AN INVESTIGATION OF PARTIAL DISCHARGE INCEPTION VOLTAGE IN AIR AND SF_6 GAS by Shri PARTHA HALDER has been carried out under my supervision and this report has not been submitted elsewhere for a degree

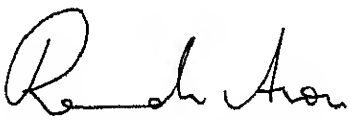

Dr Ravindra Arora
Professor
EE Department
IIT Kanpur INDIA

Department of Electrical Engineering
Indian Institute of Technology
Kanpur 208016

Dedicated to my

Mother

ACKNOWLEDGEMENT

I wish to acknowledge my deep sense of gratitude to Dr Ravindra Arora who has initiated me into this problem and provided the necessary education guidance and encouragement at every step without which this work would not been possible

I wish to thank my friend Sudhir Kr Singh R I Kamal and K Pahari for their help valuable suggestions and support throughout the work

My sincere thanks to Mr S V Ghorpade and Mr Ram Avtar of our high voltage laboratory Mr B Kumar Mr Gujral Mr Sairam of Glass Blowing Lab and ACES Lab for their help and assistance in fabricating and setting up the test apparatus at numerous occasions

At the end I wish to thank my Father Mother Sisters Sailendra Tusherda and my wife for their loving attention and cooperation and understanding for my long and odd hour absence from the house

January 2001 Partha Halder

Abstract

Stable partial discharges in dielectrics take place only under extremely nonuniform field conditions In enclosed gaseous dielectrics for example gas insulated system (GIS) extremely nonuniform fields are not acceptable as the resultant corona may degenerate the dielectrics It is therefore desired the Schwaiger factor must be within a limit and the field remains weakly nonuniform However if the nonuniformity in the field increased streamer corona may incept In this work the partial discharge inception voltage has been investigate in air and in SF_6 gas with the same electrode configuration system for increasing gap distance with ac power frequency voltage

Literature study revealed that a lot of work has been performed for the investigation of PDIV with pointed sharp electrodes The type of PD at such electrodes is glow corona which takes place with avalanche discharge of below critical amplification due to steep fall of potential gradient at the sharp electrodes In this work electrode configuration chosen are rod plane where the fall of potential gradient is comparatively not so steep giving rise to streamer corona with avalanche discharge of above critical amplification

Experiments in air have been performed to be able to compare the performance of needle plane and rod plane electrode system PD inception observed on needle plane electrode was at lower voltages than that of rod plane electrode These give rise to glow and streamer coronas respectively It could be observed that on varying the gap distance it does not affect the Pd inception voltage level much and the plot shows the flat characteristic in both the cases Breakdown voltages for 6 and 8 mm rod electrodes are much higher than the Pd inception voltage in air and the difference between them

increases with increasing gap distance It is also observed that audible PD i e hissing sound is produced at much higher voltage than the measured PD This concludes that PD occurs at lower voltage but human ear can realize it at higher voltage only

Experiments in SF_6 gas were performed only for measurement of partial discharge inception voltage for 6mm rod plane electrode system with variable gap distance at variable pressure Like in air in this case also PDIV characteristics were also measured to be flat When the pressure was increased the value of PDIV also increased and when the pressure was decreased then the value of PDIV also decreased It was observed that at constant pressure with increase in gap distance PDIV value increases but not too much After a certain gap distance at all pressures it was observed that value of PDIV becomes steady i e no increase in PDIV value with increase in gap distance is marginal For same gap distance whenever pressure increases PDIV also increases upto a certain gap distance It was also observed that in SF_6 at normal atmospheric pressure PDIV value is greater than that in air for the same gap distance and this value increases with increase in gas pressure So it proves that SF_6 gas has higher PDIV than that of air

Contents

LIST OF FIGURES

LIST OF TABLES

List of symbol

ı (Volt ɓ)	Alteı ɑtıı g p veı f equency volt g
BDV	B ɑk l w volt ge
n	Ceı tımeteı
dc	Dıect cuıı ent
I	Llectrıc fıeld ıntensıty
L_b	Fıeld ıntensıty ıequıred foı bıeɑkdown
E	Aveıɑge electrıc fıeld ıntensıty
L	Lıgen spɑce chɑıge
E	Extɛrnally ɑpplıed fıeld
E	Maxıı ı m fı ld ınt ns ty
$Γ_b$	Maxımum fıeld ıntensıty ıe jumed foı bıeɑkdown
I	Aveıɑge potentıɑl gı ɑdient
E_b	Intrınsıc stıength of gɑs
$Γ_ı$	Mınımum ıntensıty ıequııed foı ımpɑct ıonızɑtıon
CIS	Gas ınsulɑted system
HV	Hıgh voltage
kA	10^3 Ampeıe
kV	10^3 Volts
kVA	Kılo volt ɑmpeıe
kHz	10^3 Heız
MHz	10^6 Hεrz
Ms	Mılhsecond
Mpa	10^6 Pascal
mbɑı	10^3 Bɑr
η	Schwɑıgeı f ctor degıee of unıformıty
$η_ı$	Thıeshold degree of Unıformity
η	Attachment coefficıent
α	Ionızatıon coefficıent
α	Effectıve Ionızatıon coefficıent
Ω	Ohm
nC	Nano coulomb
p	Geometrıcɑl chɑıɑcteııstıcs
r	Radıus of most curved surface
pd	Product of pıessure and gap dıstance
PD	Partıɑl dıscharge
PDIV	Partıɑl dıscharge ınceptıon voltɑge
$U_ı$	Inceptıon voltage
U_b	Breakdown voltage
d	Gap dıstance
ns	Nano second
μA	Mıcıo ampere
pC	Pıco coulomb
X	Crıtıcal gap length
$SΓ_6$	Sulphur hexɑfluoııde gas

Chapter 1

Introduction

1.1 General Introduction

With the present trend of increasing transmission voltages and the costs world over gas insulated system (GIS) have assumed great significance These offer the advantages of higher operating voltages infrequent maintenance and less space requirement A gas insulated sub station for instance occupies one tenth the space taken by an outdoor sub station for the same operating specification To prevent from occurring corona in GIS it is essential the field to be weakly non uniform type In GIS all the high voltage components are enclosed in a compressed gas dielectric Any partial discharge in the gaseous dielectric lead to its deterioration and hence reduce its insulating properties Moreover PD gives rise to a number of by products depending upon the type of gas used some of which have been found to be corrosive and highly toxic SF_6 is a electronegative gas and some byproducts of this are toxic

Electric discharges which do not bridge the electrodes are called partial discharge In other words the type of breakdown occurs is local not global Partial discharge phenomenon produces very short duration pulses Although they are small in magnitude but they can cause progressive deterioration and ultimately failure of the insulation Therefore it is essential to investigate their performance in order to ensure reliable operation of high voltage equipment A meaningful interpretation of partial discharge measurement required in order to identify its source Therefore several methods are

iv ul ible foi partial disch ıge me isuiement used widely to detect defects in insul ition system of HV equipment as well is to inter insul ition system gi idation Due to the stochastic behavioi of this phenomenon a wide set of p ıtiıl dischaıge pulses geneıally aıe needed to evaluate the qu ility of in insulation system

Referred to a solid dielectric when the voltage across a cavity reaches the breakdown value the cavity may breakdown The voltage breakdown takes place in less than 10μ sec This is extremely short time compared to the duration of a 50 Hz sine wave and hence the voltage drop m ıy be regarded to be a step function The voltage across the cavity starts increasing until it reaches the breakdown voltage again when a new discharge occurs Several discharges may takes place during the rising part of the applied voltage Similarly on the decreasing part of the applied voltage the cavity discharge occur as the voltage across the cavity reaches the negative v ılue of the breakdown voltage In this way a groups of dischaıges oriğinate from a cavity and give rise to positive and negative current pulses on rising and decreasing voltage

1 2 Detection of discharge

The techniques of the detection of discharge are based on the energy exchange processes which take place during discharge Electrical discharge is transitory disturbance which radiates electiomagnetic acoustic and thermal energy from the discharge site Therefore these exchanges are manifested as electrical impulse current dielectric loss chemical transformation heat gas pressure sound and light There are two types of discharge detection methods non electrical and electrical methods

1 2 1 Non electrical detection method

Insulating materials are complex materials which when degraded by heat or electric action produce a very large number of electrical products in the gas liquid and solid state Electrical discharge activity within or adjacent to the insulating system also release chemical degradation products It breaks oxygen to give ozone Furthermore continuos PD activity gradually combines with the insulating materials to produce on a smaller scale the degradation products for example caused by local over heating

Sound is a longitudinal mechanical wave motion in an elastic medium and each wave is classified according to its frequency

1 Audible by human ear (frequency between 20 20000 Hz)

2 Infrasonic (below the response of human ear)

3 Ultrasonic (above the response of human ear)

1 2 2 Electrical detection methods

The primary characteristics which partial discharge detectors have in common and therefore could provide a basis for evaluation of the detector are the number of input employed the bandwidth of the detector and the method of display processing The three basic types of display are

1 The meter display

2 The direct display on oscilloscope

3 The computer driven display

Chapter 2

Electric fields and corona

This chapter covers briefly the type of electric field the type of coronas and the conditions under which these occur

2 1 Classification of electric fields

Fields can be classified as follows

1 Uniform field

2 Weakly nonuniform field

3 Extremely nonuniform field

2 1 1 Uniform field

Uniform field is considered to be an ideal field It is a subject of considerable theoretical and practical research A uniform electric field is one in which the potential distribution across the gap is uniform The electric field intensity is the same at any point in the electrode gap in the main field region However uniform fields are not possible in practice and perforce a satisfying rather than ideal solution is sought out The breakdown strength of a dielectric is maximum in this type of field An important characteristics of this type of field is that insulation breakdown takes place without any stable partial discharge preceding the breakdown In other words

$$U_i = U_b$$

(I D inception voltage) = (Breakdown voltage)

An example of this type field is between two parallel plates having suitably shaped fringes

2 1 2 Weakly nonuniform field

In this type of field the potential distribution across the electrode gap is not uniform and hence the field intensity is not the same all over the gap However the characteristics of this type of field is similar to that of uniform field in one respect that is stable partial discharges (PD) do not take place before breakdown If the voltage applied to such an electrode configuration leads to breakdown of dielectric and U and U_b are the PD inception and breakdown voltages respectively then

$U = U_b$ (For uniform and weakly nonuniform fields)

Under this conditions if E is the field intensity in a uniform field configuration E the maximum field intensity in weakly nonuniform electrode system then the field intensity required for breakdown E_b for a given electrode systems can be related as following

$E_{max} \cong E_b$

Electrode system like sphere sphere concentric spheres and coaxial cylinders generate a weakly nonuniform field provided the gap distance between them is small

2 1 3 Extremely nonuniform field

An extremely nonuniform field is one in which the potential distribution across the electrodes is highly nonuniform An example of such a field is that between point or rod and plane electrodes If the voltage applied to an equipment comprising a gaseous dielectric is high enough to result in enhanced or distorted field at a particular location say E (equipment) equal to the field intensity required for breakdown of the dielectric in uniform field (the electric strength L_b of the dielectric) PD would incept at the location having highest field intensity That is when

E (equipment) $= E_b$ (in uniform/weakly nonuniform field)

PD incept in extremely nonuniform fields On increasing the applied voltage stronger PD may occur Breakdown of the dielectric takes place only on further increasing the applied voltage Therefore

$U << U_b$

In case of solid dielectrics the PDs may cause permanent damage to the insulation leading to breakdown However for enclosed gaseous dielectrics the effect is to reduce the breakdown strength of gas due to degeneration caused by PD Every successive PD causes further reduction in the breakdown strength These PDs also give rise of byproducts depending upon the type of gaseous dielectric which may be toxic The breakdown strength of dielectrics is minimum for extremely nonuniform fields

A comparison of the types of electric field is given in table 2 1

Table 2.1

(Typical examples of η for different field configurations)

Field Classification	Uniform	Weakly Non uniform	Strongly Non uniform
Electrode Configuration	Parallel Plate 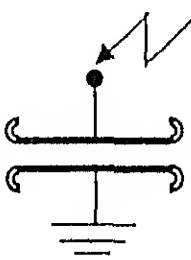	Concentric spheres 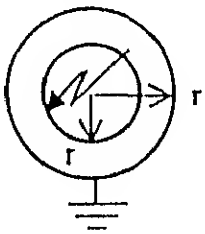 $r \geq 0.25r$	Needle plane 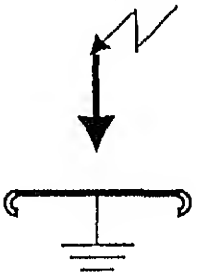
η	1.0	0.25 for air	$<<0.01$
Potential Distribution	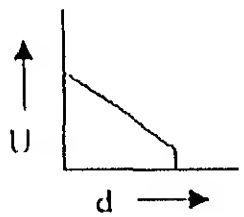	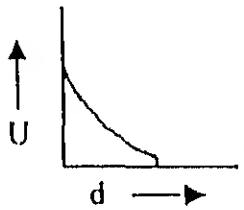	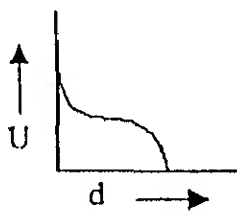
U vs U_b	$U = U_b$	$U \cong U_b$	$U_i << U_b$
Electric Field Intensity	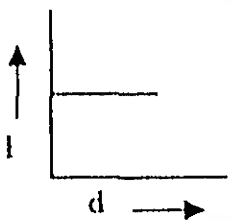	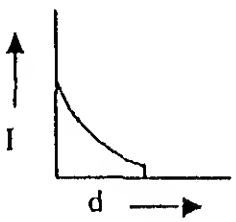	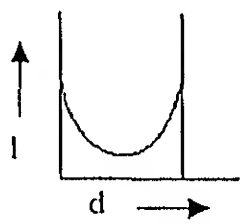

The effect of distortion of the field due to grounding of one electrode is not considered in this table

2 2 Corona

In extremely nonuniform fields at voltages much below the breakdown a stable breakdown process in the gas continued locally in the region of extreme field intensity can be maintained This is known as partial discharge (PD) and when it occurs at free electrodes in a gas it is called corona At higher working voltage (above 100 kV) it is often very difficult and economically not viable to produce apparatus free of PD at normal working voltages The knowledge of physical implication of damage caused by corona is therefore very important Depending upon the type of electrode configuration three types of coronas have been distinguished

1 Glow corona or avalanche corona
2 Streamer corona
3 Leader corona

2 2 1 Glow corona

This can be further distinguished as

1 Positive glow
2 Negative glow

Positive glow

This type of corona takes place at very sharp points in the electrode system where the fall in intensity is very steep Because of the steep fall in the field intensity the avalanche discharge process restricts itself to the tip of such electrodes and avalanche are not able to acquire adequate length of amplification The inception of further avalanche discharge is possible only

when there is a drift of space charge towards cathode accompanied with radial diffusion Then the space charge again causes an increase in fields intensity in the region away from the tip to the point of electrode to a value still sufficient for impact ionization This type of discontinuous process gives rise of impulse form of discharge current Rise time is of a few ns Time for decay to 50% value is 100 ns Peak value of current is 50 μA impulse charge is 1 pC and frequency may go 100 MHz The magnitude of mean potential gradient for breakdown of air lies between 15 20 kV/cm Optical impression of this is a weak bluish glow adjacent to the electrode and it produces hissing sound

Negative glow

In this case the avalanche develop in the opposite direction that is the avalanche head is towards the plane Hence the avalanche process limits itself within a short region and it is not able to extend further In short it can be concluded that like in case of positive polarity in case of negative polarity also a discontinuous process of discharge carries on and production of charge particles and their migration takes place The frequency of current pulse varies from a few kHz to MHz This is also called TRICHEL pulse It depends upon gap length The cathode corona appears reddish glow unlike bluish glow in the case of anode corona

2 2 2 Streamer corona

This type of corona is of greater importance in this work The transition from weakly to extremely nonuniform field is accompanied with this type of corona This type of corona takes place where fall in field at the electrode is

not so steep as for glow corona Example of such electrode systems are sphere sphere sphere plane rod plane electrodes etc

Visually the streamer discharge looks like a weakly illuminated bunch of discharge at the electrode This is accompanied by a fluttering sound which may be heard before the streamer becomes visible The streamer discharge is also accompanied with an impulse form of current This current may acquire its maximum magnitude of a few milliamperes to an ampere within nanoseconds The impulse discharge is in the range of 100 pC to 100 nC The integrated optical light appearance of streamer discharge is like a weakly illuminated bunch or more appropriately a shower of discharge Hence it is also known as bunch discharge

2 2 3 Leader corona

If the same rod plane or sphere plane electrode system is provided with a gap of the order of a meter and above the discharge trajectories are able to extend deeper into electrode gap The extended streamer phenomenon thus produced is known as a leader discharge caused by a high density of discharge current resulting in thermal ionization The leader channel is accompanied with a less bright diffused voluminous conical shower discharge from its tip This is known as leader corona and has a filamentary structure The main leader channel follows the tortuous path traced out by the leader corona ahead of the leader channel An example of unstable leader in air is lightning

Chapter 3

Theory of streamer discharge

3.1 Schwaiger factor

The Schwaiger factor (η) or the factor of uniformity or field efficiency factor was originally proposed by German scientist Schwaiger It is defined by the ratio of average field intensity to the maximum field intensity i e

$$\eta = \frac{E}{E}$$

Where E = Maximum electric field intensity in the gap

E = Average electric field intensity in the gap

This factor is a geometrical quantity related to electrostatic field analysis only Since both E and E depend upon the geometry of the electrode system the value of the Schwaiger factor also depends upon the geometry of the electrode system

3.1.1 Schwaiger factor for uniform fields

In a uniform field by definition the electric field intensity throughout the dielectric is constant As a result E and E are equal The Schwaiger factor therefore equals to unity

$\eta = 1.0$ (for uniform fields)

The breakdown voltage in a uniform field is therefore given by the simple relation $U_b = E_b \; d = U$

Where E_b = break down strength and it is not a constant its value varies with gap distance even in uniform fields

3 1 2 Schwaiger factor for weakly nonuniform fields

For a weakly nonuniform field by definition the field across the gap is non uniform Therefore

$$\eta = \frac{L}{E}$$

The value of these Schwaiger factor reduces as the non uniformity of the field increases The breakdown voltage and PD inception voltage both of which are equal for a weakly nonuniform field are given in terms of η as follows U_b/d

$$\eta = \frac{}{E}$$

Where E = Maximum electric field intensity in the gap

d = Gap distance between the electrodes

$U_b = E \; \eta \; d$

3 1 3 Schwaiger factor for extremely nonuniform fields

In this case since the potential distribution across the gap is extremely nonuniform therefore

$L << L$

As a result $\eta << 1\ 00$

For extremely nonuniform fields U_i and U_i are not equal The value of U is given by the same relation as for a weakly nonuniform field

$$U_i = E \eta d$$

However the breakdown phenomenon in extremely nonuniform fields is a vast field of research In short one can say that in this case the breakdown voltage depends upon the type of stable PD preceding the breakdown and given by

$U_b = E d$

Where E = Average potential gradient across the I D channel preceding the breakdown which could be streamer (s) or leader (l) stable PD

3 2 Schwaiger factor limits

The transition from weakly to extremely nonuniform field is accompanied with the onset of stable streamer corona The corresponding value of the Schwaiger factor at which this transition occurs is known as the Schwaiger factor limit and is denoted by η_i With the emerging importance of GIS

high voltage transmission networks across the world this concept assumes added importance

The reciprocal of η is denoted by f which represents the degree of nonuniformity of an electric field a concept also introduced by some authors in the literature Schwaiger further introduced p a geometrical characteristics for electrode configuration and established that it is possible to represent η as a function of p

$$p = r+d / r \qquad (1 < p < \eta)$$

And $\eta = f(p)$

Where

r = The radius of the most curved enveloping electrode

d= Smallest gap distance between the two electrodes under consideration

3 3 Development of streamer discharge

The growth of charge carriers in an avalanche in uniform field E_0 is exponential however this hypothesis is valid only as long as the electric fields due to the space charges of the electron and ions are negligible compare to the applied electric field E_0 This is true so long as the gap distance d between electrode is very small If the distance increased the avalanches are able to acquire bigger size developing stronger space charges When the electron space charge concentration exceeds $\cong 10^7$ to 10^8 the electron at the head and the ions at the tail of an avalanche find themselves

in a state of enhanced field Under this condition the ionization proceeds at a higher rate at the front and the tail of the avalanche but lower rate at the center At this stage the rate of advancement of the avalanche towards the anode increases by generation of fresh avalanches because of the increase in the field intensity at the upper region The fresh avalanches are produced by new electrons in the vicinity of the primary avalanche These new electrons could be produced by photo ionization caused by the primary avalanche The avalanche thus formed mainly at the head of the primary avalanche are known as secondary avalanche This development is known as anode directed streamer Simultaneously at the tail of the primary avalanche a favorable condition arises due to the cathode directed streamer Obviously it requires a sufficient number of electrons also at the cathode side of the primary avalanche to develop into cathode directed streamer

3 4 Breakdown by streamer discharge

The streamer breakdown mechanism describes the development of spark breakdown directly from a single avalanche The space charge developed by the avalanche itself due to the rapid growth of charge carriers transforms it into a conducting channel As describe by Raether it is the eigen space charge which produces the instability of the avalanche The streamer means a ribbon attached at one end and floating or waving at the other which appears to be a set of waves ripples moving forward

The approximate calculations of the conditions required for the same charge field of avalanche E to be able to acquire the magnitude of the order of the externally applied field F_0 confirmed that the transformation from the

avalanche to streamer began to develop from the head of an electron avalanche when the number of the charge carriers increased to a critical value $n_0 = e^{\alpha} \cong 10^8$

For an avalanche initiated by single electron in a uniform field this corresponds to a value

$$\alpha x = \alpha d = \ln 10^8 \cong 20$$

x the length of avalanche = Critical length of the electrode gap d this means that the streamer mechanism is possible only when $d \geq x$ On the basis of experiment results and some simple assumption Raether developed the following empirical formula for the streamer breakdown criterion

$$\alpha x = 17.7 + \ln x = \ln E / E_0$$

The condition for transition from avalanche to streamer breakdown assumes that as eigen space charge field approaches nearly the applied field ($E \cong E_0$) then this equation becomes $\alpha x = 17.7 + \ln x$

The minimum value of αx required for breakdown in a uniform field gap by streamer mechanism is obtain on the assumption that the transition from avalanche to streamer occurs when an avalanche of critical size just extends across the gap d then

$$\alpha d = 17.7 + \ln x \cong 20$$

Thus the condition $x = d$ gives the smallest value of α to produce streamer breakdown where d is given in cm

3 5 Breakdown in uniform and weakly nonuniform fields with SF_6 insulation

Townsend's theory of development of avalanche was in air basically an electropositive gas Negative ions like positive ions are too massive and slow to produce collision Hence analogues to the ionization coefficient α an attachment coefficient η is introduced η is the number of attaching collisions made by one electron drifting 1 cm in the direction of the field The ionization by electron collision is then represented by the effective ionization coefficient ($\bar{\alpha} = \alpha - \eta$) Like α / p $\bar{\alpha} / p$ is also a function of E/P figure 3 1 shows the experimentally measured values of $\bar{\alpha}$ for varying E/I in uniform field From these measured values the following relationship can be derived

$$\bar{\alpha} / p = K[E/p - (E_b/p)_1] \qquad (1)$$

Where

K – a constant and equal to 27 kV^{-1} representing the slope of the line $(E_b/p)_1$ = 890 kV / cm MPa represents the intersection of the line with abscissa And p = Pressure in MPa at normal temperature 0 = 20 C

In order that breakdown takes place α must be greater than zero which in turn is the fulfillment of the condition that E/I is greater than $(E_i/I)_1$ The magnitude of $(E_b/p)_1$ represents the inherent relative strength of the gas Field intensity E_{b1} given by the relation

$E_b = (E_b/p)_1 \cdot p = 890\ p$ kV/cm is known as the intrinsic strength of the gas The breakdown of SF_6 gas in uniform fields for small gap distances is

achieved by the generation of series of avalanches as described by Townsend's mechanism For higher values of the pressure and gap spacing (pd) streamer breakdown mechanism is observed The breakdown criterion for higher gas pressure (or product of pd) are based upon the critical number of the electrons n produced in the avalanche The critical number of electrons in an avalanche is achieved in the field direction when it acquires a critical length x which should be shorter than the gap length d In practice the gap spacing in weakly nonuniform fields are more of interest For such gap spacing the breakdown criterion of the streamer mechanism is extended taking into account the attachment coefficient of electronegative gas Beginning with a single electron initially the number of charge carriers in an avalanche considering electron attachment in weakly nonuniform field is given by

$$n = \exp \int_0 \bar{\alpha}\, dx$$

and for growth of an avalanche which gives rise to initiation of a streamer

$$n = n \quad = \exp \int_0^{x \quad d} \bar{\alpha}\, dx$$

$$\text{or } \int_0^{x \quad d} \bar{\alpha}\, dx = \ln n \quad \cong 20 \qquad (2)$$

From equation (1) & (2) breakdown voltage for SF_6 in weakly nonuniform field configuration can be estimated theoretically Breakdown under these conditions takes place without any stable PD [1] It is tacitly assumed that breakdown occurs when the number of electrons n is an electron avalanche reaches a critical value n Actual value of n is not known but the criteria $n = 10^8$ is considered to be valid irrespective of the specific conditions for the weakly nonuniform field In uniform or in weakly nonuniform fields x

will be synonymous with gap length d However in extremely nonuniform fields x is the distance from the electrode along the field line in question to the point beyond which the growth of the avalanche ceases i e to the point which $\bar{\alpha} = 0$

Owing to the random nature of the initial stages of the avalanche growth i e for $x < x_1$ Where x_1 is the length of critical amplification of avalanche in extremely nonuniform field The value of x_1 will vary considerably for a series of single avalanches developing along the same path Consequently for any value $x > x_1$ a maximum value $n(x)$ for n(x) can be obtained for a minimum value of x_1 Therefore for a finite avalanche length the onset of the breakdown will be associated with the avalanche processing the largest number of electrons The criterion for the onset of breakdown can be thus expressed in the following form $x = n(x)$ the breakdown will occur when the integral attains a certain value K Thus the streamer criterion can be written as

$$\int_0 \bar{\alpha}(x)dx = K \qquad (3)$$

It is evident that this criterion is strictly empirical In the literature K is often given the value 18 this being the natural logarithm of the value generally assumed for x viz 10^8

So far it has been tacitly assumed that the electric field L(x) varies monotonically with x between 0 and x such that the integral of $\bar{\alpha}$ would also be a monotonically varying function of x However in some situation E(x) will not vary monotonically within the interval $x_1 < x < x$ An example of such an axial field is between the two spheres for which the ratio of gap

length d to the sphere diameter D such that x d which is a typical example of weakly nonuniform field In such situations the application of the streamer criterion is valid if for all values of x in the interval $x_1 \le x \le x$

$$\int_{x_1} \bar{\alpha}(x)\,dx \ge 0 \qquad (4)$$

Since this implies that n(x) will never be less than $n(x_1)$ thus ensuring swarm condition i e the growth of avalanche discharge one above the other However since the value of x_1 is unknown equation (4) with reference to nominal calculations is of little practical value As a substitute the less rigorous condition

$$\int_{0} \bar{\alpha}(x)\,dx > 0 \qquad (5)$$

can be used as an indication for the validity of my calculations It should however be noted that fulfillment of (5) does not automatically imply swarm conditions [11]

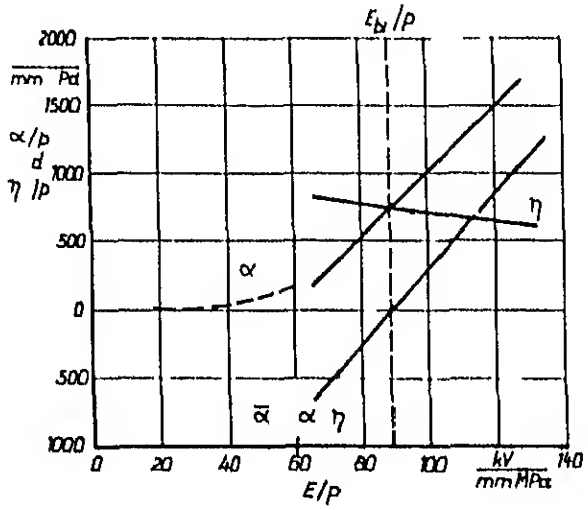

Figure 3 1 The ioniz tion and attachment coefficient of SF6 as a function of reduced field intensity [1]

3 6 Positive rod plane electrode (positive streamer corona)

When the avalanche has grown to its critical size the following equation must hold good

$$\int_0^{x_c d} \bar{\alpha}\, dx = \ln n / n_0 \cong 20$$

Where x is the length of an avalanche when it acquires its critical amplification For the avalanche to develop under this condition the electric field intensity must however remain in the field region above E_i the minimum field intensity required for impact ionization The fig 3 2 shows that the electrons at the head of the avalanche are absorbed by the positive rod electrode leaving positive space charge behind which weakens the field When the avalanche acquires its critical stage there is a strong concentration of positive space charge till upto the tail of avalanche An increase in field intensity towards the tail of avalanche results due to the presence of a weak negative space charge produced at the front of the next avalanche which is formed by photon emission from the avalanche head and resultant magnitude of the field intensity increases higher than E_i This process continues so long as a subsequent avalanche started by photo ionization falls in the field region above E_i inspite of basic field decreasing below this level Since the positive charge carriers being heavier particles do not move themselves much the process is comparable to the movement of a wave In fact the numerous avalanche being together the whole process is a continuous development of large number of space charge trajectories These spread in space charge around the rod electrode in the main field direction The negative streamer corona development is similar except that

the direction of the avalanche is opposite The development of streamer corona with ac power frequency voltage is combination of the two

3 7 Distinguish between breakdown with stable and instable streamer

A distinction between breakdown with stable and instable streamer can be made interms of the degree of uniformity of the field Taking a positive sphere sphere electrode with increasing gap distance At small gap distance weakly nonuniform field exists On applying voltage to achieve the required

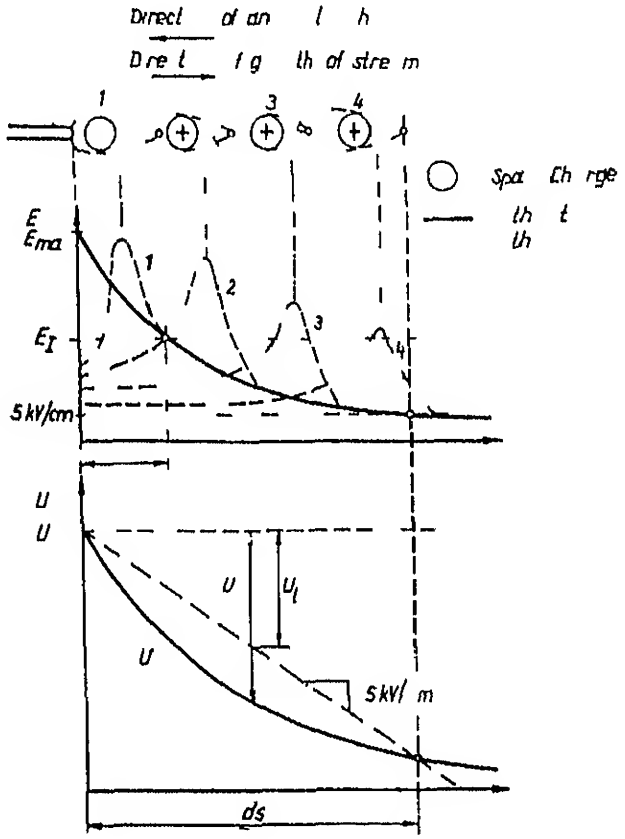

Figure 3 2 Schematic of streamer discharge in front of a positive rod electrode with variation in field and potential as a consequence of space charge [1]

maximum field intensity for breakdown E_i the inception of streamer discharge immediately leads to an abrupt breakdown in region A in fig 3 3 no I D occur in this region On increasing the gap distance the field becomes more non uniform Beyond the region A a condition is reached when streamer discharge after incepting on the electrode are not able to extend immediately upto the opposite electrode In contrast to A in the region B stable streamer partial discharges take place The border line between

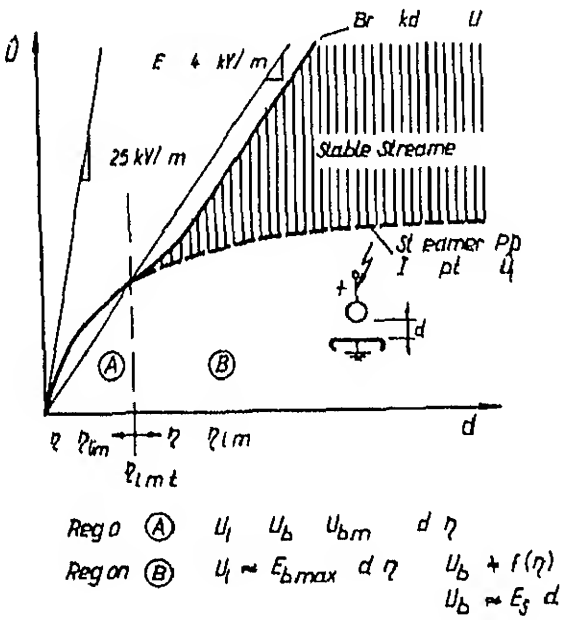

Figure 3 3 Threshold curves showing breakdown with stable streamer for positive sphere plane electrode configuration [1]

these two regions is described as η_{II} In the region A $\eta > \eta_I$ whereas in region B $\eta < \eta_{II}$ The threshold degree of uniformity η_{II} is the point where the maximum field intensity at the tip of the rod is sufficient for the breakdown to take place with stable streamer discharge η_{II} also represents the transition from the weakly nonuniform and the extremely nonuniform

fields The position of the line representing η_1 is the transition from weakly to extremely nonuniform field In region B the LD inception voltage U in terms of the electrode geometry can be estimated but not the breakdown voltage The magnitude of the breakdown voltage in the region B primarily depends upon the average potential gradient required for the growth of streamer E which is 7kV/cm (peak) for air on applying ac power frequency voltage [9]

Chapter 4

BEHAVIOUR OF SF_6 GAS

4.1 Introduction

Sulphur hexafluoride was first produced in 1900 by French scintist Moissan Lebeau by direct fluorination of sulphur In the beginning it was mainly used as a dielectric in atomic physics During late 1950 it found application in high voltage circuit breaker Ever since its application in power system has been continuously increasing

Spark breakdown in gaseous media represents a fugitive phenomenon often studied with high voltage impulse long enough in duration to allow its formation and development

SF_6 is widely used in electric power apparatus such as gas insulated switch gears (GIS) not only because of its superior dielectric propeities but also its chemically inert and nontoxic characteristics and also good heat transfer properties

Since SF_6 gas insulated power apparatus like gas insulated switchgear (GIS) have been widely used in high voltage substation of electric power transmission and distribution It is strongly needed to investigate the operational reliability of the apparatus For example insulation defects like metallic particles in GIS would be a cause of partial discharge (PD) and could lead to dielectric breakdown Thus for the stable operation of GIS it is very important to diagnose the insulation condition in service and to predict the breakdown using PD detection technique Therefore it is crucial to clarify the PD mechanism the SF_6 and to develop the breakdown prediction technique in GIS Under ac voltage application however space charges generated by PD show complicated behaviour and have an influence

to I D themselves due to the temporal change of the instantaneous value and the polarity of the applied voltage Thus it is important to investigate the I D mechanism under ac voltage

4 2 Physical properties of SF_6 gas

In a SF_6 molecule six fluorine atoms arrange themselves uniformly like an octahedron on a central sulphur atom An excited sulphur atom can therefore form six stable co valence bonds with the strongly electronegative fluorine atoms by sharing the pair of electrons Amongst halogens the fluorine elements and sulphur atom have very high coefficients of electronegativity of the order of 4 and 2 5 respectively This coefficient is a measure of the tendency to attract electrons of the other atoms to form dipole bondage The rigid symmetrical structure small binding distance and high binding energy between atoms of a SF_6 molecule provide it a high order of stability With the result SF_6 gas properties are near that of rare gases at relatively low temperatures Thermal dissociation of highly purified SF_6 gas begins at extremely high temperatures (above 1000K) Such high temperature in power system occurs only in the electrical arcs Even at continuous temperature upto about 500K neither thermal decomposition of SF_6 nor its chemical reaction with other materials have been reported Further SF_6 is a nontoxic colourless and odourless gas

The density of gases increase with relative molecular mass As the molecular mass of SF_6 is quite high (146) it has a high density Because of high density the charge carriers have a short mean free path This properties along with the properties of electron attachment i e electronegativity and

high ionization energy results in high dielectric strength of SF_6. Some important physical properties are brought together in table 4.1 [1]

Physical properties of SF_6

Property	Physical conditions	Symbol	Unit	Value
Relative permitivity	0.1 MPa 25 C	ϵ	—	1.002 1.81±0.02
Dielectric loss tangent	0.1 MPa 51 C (liquid)	tanδ	—	$<5\ 10^{-6}$
Critical temperature	—	θ	C	45.5
Tripple point	P = 0.22MPa	θ_t	C	50.8
Sublimation point	—	θ_s	C	63.8
Specific heat capacity	At 10 C and constant P = 0.1 Mpa at 10 C and constant volume	C_p C	J/mol K J/mol K	5.13 4.06
Heat conductivity	30 C	—	J/cm sK	0.82×10^{-5}
Heat transition number	—	—	J/cm^2 sK	0.44×10^{-5}

Table 4.1

Other properties of SF_6 gas

Data for I=0 1MPa		Dielectric strength θ=20 C	Relative molecular mass	Density θ=20 C	Mean free path of electrons	Ionization energy	Normal condensation temperature
Gas	Symbol	E_b (kV/Cm)	M	ρ (kg/m^3)	λ (μm)	W_I (eV)	θ (C)
Sulphur hexafluoride	SF_6	89	146	6 39	0 22	15 9 to 19 3	63

Table 4 2

4 3 Electron attachment properties of SF_6 gas

Some atoms or molecules in their natural gaseous state have an affinity to acquire free electron and form a stable negative ion This property of negative ion formation is known as electron attachment or electron affinity It has been proved that the atomic or molecular gases having electron affinity lack one or two electrons in their outer shell and hence are known as electronegative gases For example the halogens(F Cl Br I) have one electron missing in their outer shells whereas O S Se have two electrons less in their outer shells

For attachment of an electron to a neutral molecule the electron must have a certain minimum kinetic energy This energy is the order of 1eV very low compared to the energy required for impact ionization For a negative ion to remain stable for some time its total energy must be lower than that of a neutral molecule in the ground state This difference in the energy levels is

known as electron affinity of the molecule It is released as a quantum of kinetic energy on attachment

There are so many process of negative ion formation

1 Radiative attachment process

2 Collision attachment process

3 Dissociative attachment process

The attachment process in SF_6 gas is characterised with dissociative attachment It is caused by an electron impact separating the molecule into a neutral particle and a negative ion having a similar mass as the neutral gas molecule

4 4 Breakdown in extremely nonuniform field in SF_6 gas with stable PD

Experimental investigations have revealed that in compressed gas insulated nonuniform electrode arrangements the inception of PD not only depends upon electrode geometry but it is also strongly affected by the gas pressure From the practical point of view it is therefore important to know the extent of applicability of Schwaiger relation for estimating the PD inception The pressure dependent limiting uniformity factor η_i for SF_6 gas is shown in fig 4 1 In the region $\eta > \eta_i$ no stable PD occur whereas in the region $\eta < \eta_i$ stable PD are observed before the breakdown As shown in fig 4 2 PD measurements were made on a point plane electrode system with increasing gap distance in SF_6 at atmospheric pressure On applying a direct voltage lower PD inception levels were measured for negative polarity point electrode than for positive polarity As in the case of atmospheric air in SF_6 gas too a compact glow discharge is observed at the sharp point electrode

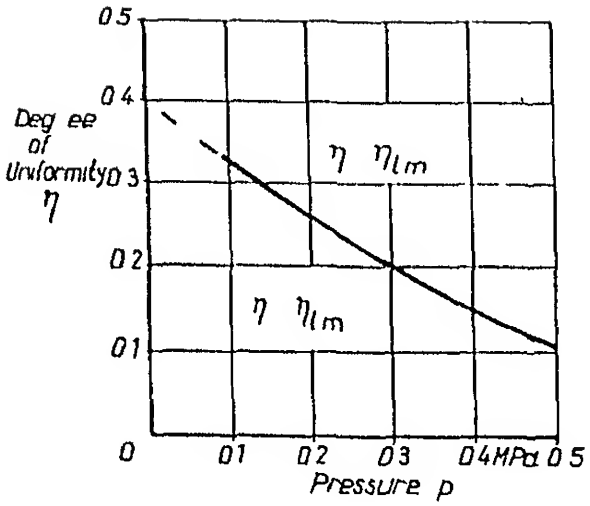

Fig u 4 1 I re s u depei d nt limiti g d gice f u i f i nity foi el t od onf gu atio m SF_6 [1]

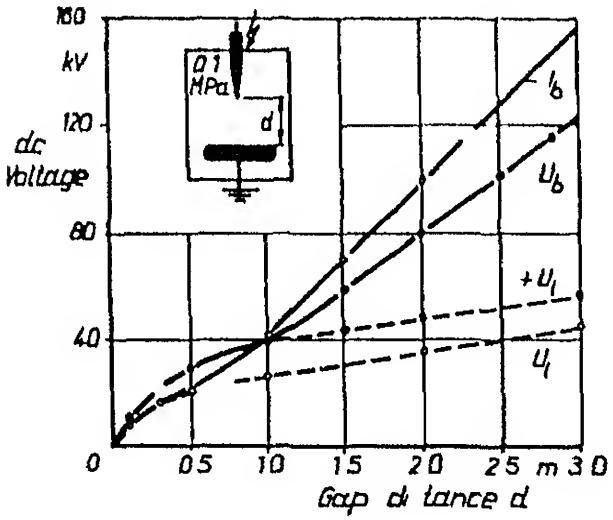

Figure 4 2 Breakdown with direct voltage on a point plane electrode in SF_6 gas with increasing gap distance [1]

in extremely nonuniform fields The nature of the discharge current is the same as in the case of air Stronger discharge current pulse are measured with negative polarity point electrode than with positive polarity The field

equalizing effect of the space charge is also stronger with negative polarity point electrode requiring high voltages for accomplishing inception and breakdown voltages are valid for all types of voltages in SF_6 gas [1]

4 5 Decomposition of SF_6 gas in equipment

The increased application SF_6 in gas insulated switchgears / substations (GIS) compressed gas insulated transmission line (CGIT) electrostatic accelerators and X ray equipment etc have led to growing concern and investigation of the mechanism of SF_6 decomposition and effects of decomposition products on the equipment In the presence of corona (PD) spark breakdown and electric power arc SF_6 decomposes into lower oxi fluorides of sulphur These may react with the electrode or gas impurities or other solid dielectrics to form a number of chemically active products Although SF_6 is chemically inert and nontoxic the decomposition products of SF_6 are known to be toxic and corrosive The accumulation of decomposition products in the equipment has caused concern regarding personnel safety and material capability The decomposition products of SF_6 are greatly influenced by gaseous impurities In industrial grade of SF_6 the typical impurities are CH_4 N_2 O_2(air) and H_2O The gaseous impurities are generally introduced during filling and partly due to the decomposition of moisture into the dry SF_6 after filter

The decomposition of SF_6 can be caused by three different fundamental process electronic and thermal process are dominant resulting in the formation of stable products Electronic and thermal processes both can occur in discharges such as spark breakdown and power (heavy current)

ues The decomposition of SF_6 due to PD is mainly under non thermodynamic equilibrium conditions where the temperature is higher than the gas temperature [1]

4 6 Limitations and greenhouse effect of SF_6 gas

SF_6 is used in power electric apparatus due to its superior insulation strength However it is known that breakdown strength in SF_6 under nonuniform electric field like metallic particle condition is extremely susceptible leading to be lower break down voltage It has also high liquefied temperature SF_6 is also a very potent and persistent green house gas that contributes the global climate change [7]

4 6 1 Green house effect

EPA s (United State Environmental Protection Agency) concern about global climate change is rooted in science Over the past century the average temperature of the planet has increased roughly one degree Fahrenheit and the eleven warmest years on record have all occurred since 1980 The primary cause of this rise in global temperature is the increase in anthropogenic emission of green house gases e g CO_2 CH_4 perfluorocarbons (PFCs) hydrofluorocarbons (HFCs) nitrous oxide (N_2O) & SF_6 As these gases accumulate in atmosphere they act like a blanket warming the planet by trapping heat that otherwise would be radiated from the earth back to space The burning of fossil fuel by power plants for energy and fuel used for transportation is the primary source of emission concerns about global warming Warmer temperature could lead to

increased frequency of extreme weather events such as heat waves and droughts Changes in precipitation and increased evaporation from higher temperatures could affect quality and quantity of water posing threats to hydropower irrigation fisheries and drinking water Agriculture and forest ecosystem may get hard hit by shifts in precipitation patterns and growing zones Sea level could rise placing heavily populated coastal regions in Jeopardy Human health might be harmed and there may be increase in the rate of heat related mortality and in the potential for the spread of diseases such as malaria yellow fever and encephalitis

Emission of SF_6 occur by three mechanisms

1 Leaks due to failure of mechanical seals
2 Accidental releases due to break in the enclosures
3 Procedural release such as during gas transfer operations or maintenance checks

If all SF_6 equipment leaked at 1% or less annually those emissions would still be a cause for concern for two reasons first SF_6 is an extremely potent greenhouse gas with a global warming (GWP) potential of 23900 over a 100 year period SF_6 is 23900 times more effective in trapping infrared radiation than an equivalent amount of CO_2 A relatively small amount of SF_6 can have a significant impact on global climate change Second SF_6 is very persistent with an atmospheric lifetime of 3200 years As the gas emitted accumulates in an essentially undegraded state for many centuries Therefore a 1% annual leak rate for a piece of equipment in service thirty years roughly equivalent in terms of global warming potential to the instantaneous release of 30% of the equipment gas However a recent study has revealed that the cause of present Global warming is due to increased solar flare activity on the sun emitting more heat to earth

Chapter 5

Experimental set up

5.1 Introduction

Gas insulated power apparatus and switchgears have been widely used in electric power transmission and distribution systems. However the insulation performance of SF_6 gas deteriorates under inhomogeneous electric fields which is often caused by metallic particle contamination. In such cases PD occurs where the electric field is concentrated and finally PD would lead to flash over. Although many PD detection methods have been developed most method have not taken into account the PD generation and suppression mechanisms especially under ac condition. This is because the space charge behavior is very much complicated under ac condition and the PD characteristics are strongly influenced by space charges. From this point of view detailed investigation of PD mechanisms under ac condition is strongly needed for insulation diagnosis and reliable prediction of the lifetime. To generate different partial discharge sources in the laboratory a suitable measuring circuit has to be used. This chapter explains how partial discharge have been measured in the laboratory. The description of the electrode system prepared and the equipment used for the measurement as well as the circuit utilized for recording of partial discharge patterns are presented in present chapter.

5.2 Measurement circuit

Electric pulse detection is the main target in this thesis. The following circuit diagram measured the partial discharges and shown in fig. 5.1. This method

4 7 Conclusion

Because of its chemical stability and high dielectric strength (90kV/cm/bar) and its excellent arc quenching properties the SF_6 gas has been almost universally employed in high voltage gas insulated equipment and circuit breakers A major limitation of its relative liquification temperature (−33 C at 40 kPa) the apparatus insulated with pure SF_6 becomes unsuitable for use in cold regions It is crucial to clarify the PD mechanism in SF_6 and to develop the I D prediction technique in GIS Under ac voltage application however space charges generated by PD complicate the behavior and have an influence on PD themselves due to the temporal change of the instantaneous value and the polarity of the applied voltage Thus it is important to investigate the PD mechanism under ac voltage application From these point of views investigation must be made under ac voltage application in SF_6

Chapter 5

Experimental set up

5.1 Introduction

Gas insulated power apparatus and switchgears have been widely used in electric power transmission and distribution systems. However the insulation performance of SF_6 gas deteriorates under inhomogeneous electric fields which is often caused by metallic particle contamination. In such cases PD occurs where the electric field is concentrated and finally PD would lead to flash over. Although many PD detection methods have been developed most method have not taken into account the PD generation and suppression mechanisms especially under ac condition. This is because the space charge behavior is very much complicated under ac condition and the PD characteristics are strongly influenced by space charges. From this point of view detailed investigation of PD mechanisms under ac condition is strongly needed for insulation diagnosis and reliable prediction of the lifetime. To generate different partial discharge sources in the laboratory a suitable measuring circuit has to be used. This chapter explains how partial discharge have been measured in the laboratory. The description of the electrode system prepared and the equipment used for the measurement as well as the circuit utilized for recording of partial discharge patterns are presented in present chapter.

5.2 Measurement circuit

Electric pulse detection is the main target in this thesis. The following circuit diagram measured the partial discharges and shown in fig. 5.1. This method

is based on the measurement of the circuit impulses caused by a discharge in the test object From this circuit diagram we can see that the test sample is grounded directly The measurement set up consists of high voltage source test sample coupling capacitor measuring impedance filter and amplifier digital storage oscilloscope and a personal computer The high frequency partial discharge pulses are measured through coupling capacitor grounded through an impedance The measured pulses are first filtered and amplified and then digitized from the analog form through a digital storage oscilloscope and sent to the personal computer The specification of each component of the measuring circuit is given below

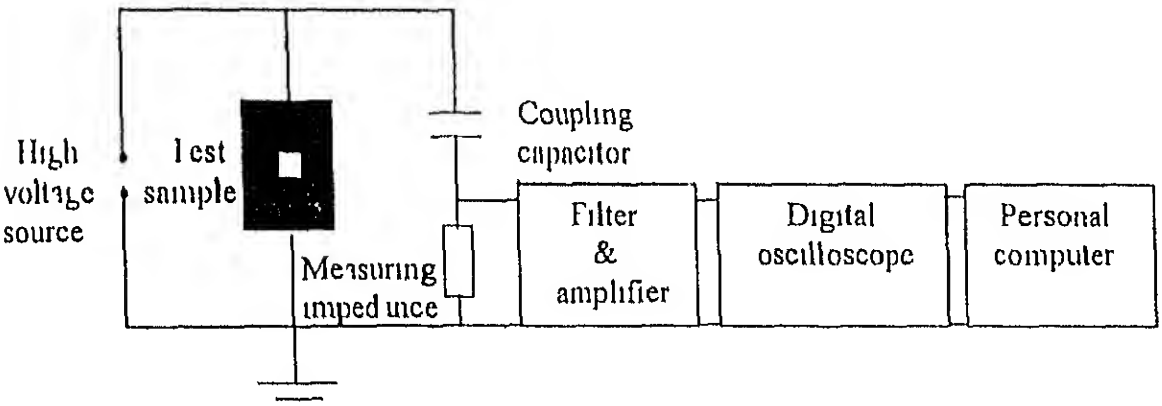

Figure 5 1 Partial discharge detection circuit

5 2 1 High voltage supply

A variable high voltage was obtained from a 100 kV 50 kVA ac power frequency PD free transformer The high voltage terminal of the transformer was connected to an 1100 pf 100 kV PD free high voltage condenser with

the help of 1 7 5 cm diameter aluminum pipe The measurements of partial discharge pulses were taken from the low voltage end of this coupling capacitor Both the test transformer and the coupling capacitor high voltage terminals are provided with domes in order to prevent any partial discharge upto their rated voltages These were verified as being partial discharge free up to 95kV The coupling capacitor was connected to the test sample with the help of 3 cm diameter flexible conduit pipe which has a bell shape end to prevent the Partial Discharge at the connecting end

5 2 2 Measuring impedance

A RLC parallel circuit was used as the measuring impedance It contains an inductance which is used to suppress the 50 Hz alternating current and its harmonics such that the unbiased signal of partial discharge can be applied to the measuring circuit With the help of a variable resister in the range of 150 Ω and 12 kΩ the measurement sensitivity can be selected for the corresponding test requirement Also it contains a spark gap a charge eliminator and four diodes for over voltage protection This impedance was also used to facilitate pulse observation since the inductance and capacitance produced an oscillatory response which persists much longer than the initiating pulse

5 2 3 Filter and amplifier

Since the partial discharge pulses are in general a series of very short duration pulses having a magnitude of the order of millivolts superimposed on power frequency these have to be filtered and amplified An electric

filter is often a frequency selection circuit that passes a specific band of frequencies and blocks or attenuates signals of frequencies outside this band Filters may be classified in a number of ways

a Analog or digital

b Passive or active

c Audio or radio frequency

Analog filters are designed to process analog signals This is natural when dealing with signals that is continuos However digital filter process deals with discrete signals Depending upon the type of the elements used in their construction filters may be classified as passive or active Elements used in passive filters are resistors capacitors and inductors Active filters on the other hand employ transistors or operational amplifiers in addition to the resistors and capacitors The type of elements used dictates the operating frequency range of the filter For example RC filters are commonly used for the audio or low frequency operation whereas LC filters are employed at radio frequency or high frequency In audio frequency inductors are often not used because they are very large costly and may dissipate more power An active filter offers the following advantages over the passive one

(i) Gain and frequency adjustment flexibility Since the operational amplifier is capable of providing a gain the input signal is not attenuated as in the case of passive filters In addition an active filter is easier to tune or in adjustment

(ii) Reduce loading problem Because of the high and low output resistances of the operational amplifier the active filters do not cause excessive loading to the source

(iii) Cost effectiveness Typically active filters are more economical than passive filters This is because of the availability of variety of chapter operational amplifier and absence of inductors

The most commonly used filters are low pass filters high pass filter band pass filter band reject filter and all passes filter In this study since the measured partial discharge pulses have to be filtered from the low frequency harmonics and the very high frequency interface an analog active wide band pass filter was used Simple cascading high pass and low pass sections can find a wide band pass filter To obtain a ± 20 dB/decade band pass filter first order high pass and low pass sections are cascaded For a ±40 dB/decade band pass filter second order high pass and second order low pass sections are cascaded In this study first order high pass and low pass sections have been used For the low pass filter the higher cut off frequency was 400 kHz Whereas for the high pass filter the lower cut off frequency was 40 kHz The filter was constructed having the operational amplifier as the active elements Selecting a capacitor C and then calculating the value of resistance R with the relation did the design of low pass filter

$$R = \frac{1}{2 \pi f_H C}$$

Where f_H is the cut off frequency The schematic diagram of the low pass filter is shown in figure 5 2 The value of R_I and R_F determine the pass band gain as following

$$A_f = 1 + R_f / R_1$$

For the low pass filter the capacitor C was selected as 0.1 nF and the resistor R as 0.4 kΩ. The high pass filter was constructed simply by interchanging the position of the resistor R and the capacitor C used in the low pass filter. The schematic diagram of the high pass filter is shown in fig. 5.3. The values of R and C for low cut off frequency of 40 kHz were selected as 4 kΩ and 1nF respectively.

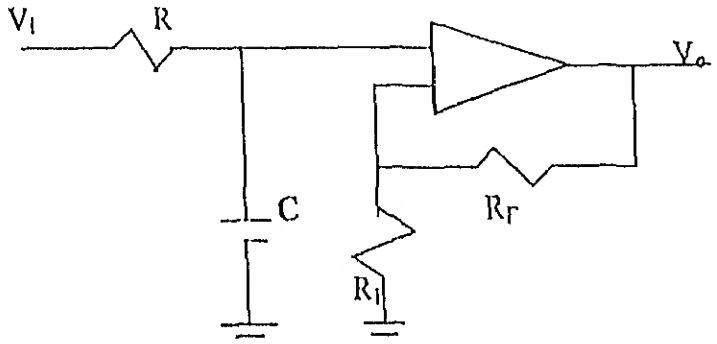

Figure 5.2 Low pass filter with 400 kHz cut off frequency

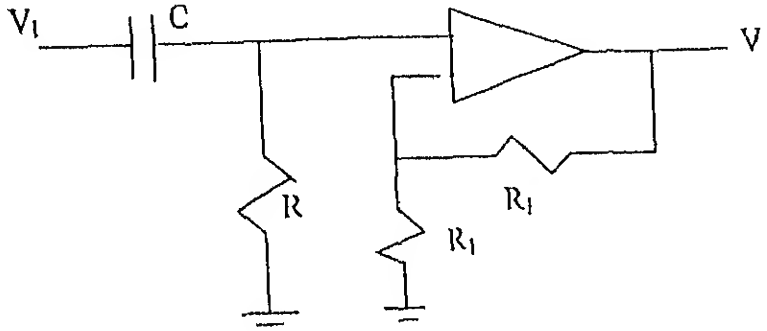

Figure 5.3 High pass filter with 40 kHz cut off frequency

Fig 5 4 shows the effect of using filter and amplifier on the measured partial discharge pulses Channel 1 (CH 1) shows the input of the filter and the amplifier while channel 2 (CH 2) shows the output pulses The effect of the filter and amplifier can be noticed by comparing the scales of the two channels (CH 1 was set at to 0 2 V /cm while CH 2 was adjusted to 5V/cm)

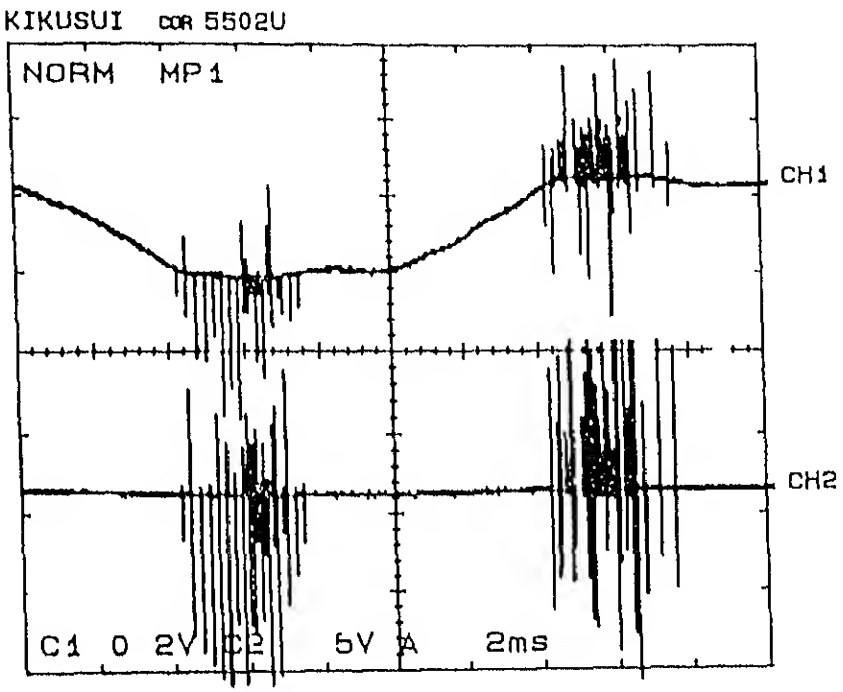

Figure 5 4 the effect of filter and amplifier on the measurements
(CH1 The partial discharge pulses before the filter and amplifier
(CH2 The partial discharge pulses after the filter and amplifier)

5 2 4 Digital oscilloscope

Kikusui COR 5502U oscilloscope was used for digitizing and storing the I D pulses The oscilloscope has two saving memory units each having a 4k word capacity The maximum sampling rate of the oscilloscope is 100MS/s

(10ns) The signals from both the channels can be digitized whereas each channel has its own A/D converter The input analog signal is converted in to digital form by A/D converter and its output is copied into the acquisition RAM Then the data is transferred from the acquisition RAM to the display RAM The oscilloscope displays it on the CRT screen with the help of D/A converter After displaying the wave form for about 1 sec the next data acquisition cycle starts The IFO2 COR interface which is best on the standard RS 232C link was attached to the oscilloscope RS 232C is used for communication between oscilloscope and peripheral terminals at relatively slow transmission Alphanumeric communication is most frequently done by using 7 bit ASC II code Generally ASC II can be transmitted in either parallel 8 bit group (8 separate wires) or as a serial string of 8 bits one after the other over a single line RS232C was used for serial transmission Using full handshaking did communication between the computer and oscilloscope Since the oscilloscope was working in the triggering mode the computer sends the triggering commands to the oscilloscope and then wait for a massage from oscilloscope that the wave form has been captured and digitized and it is ready for transfer After transferring the digitized waveform to the computer another triggering command is given to the next waveform In the measurement setup these waveforms were the partial discharge pulses superimposed on the power frequency cycle The number of required cycle for measurement could be controlled by the computer Since the partial discharge pulses occur at the maximum rising or maximum decreasing parts of the applied high voltage only and the pattern of the pulses at these parts are different it is required to study each part individually Therefore a RC circuit was used to shift the triggering signal by 90 degree to locate the partial discharge pulses around

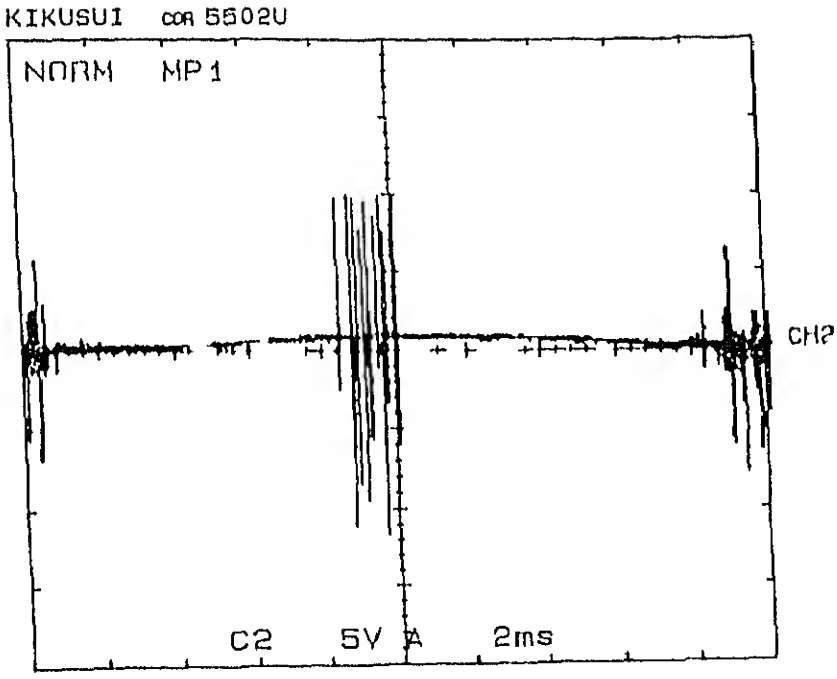

Fig 5 5a The partial discharge pulses before the phase shifter

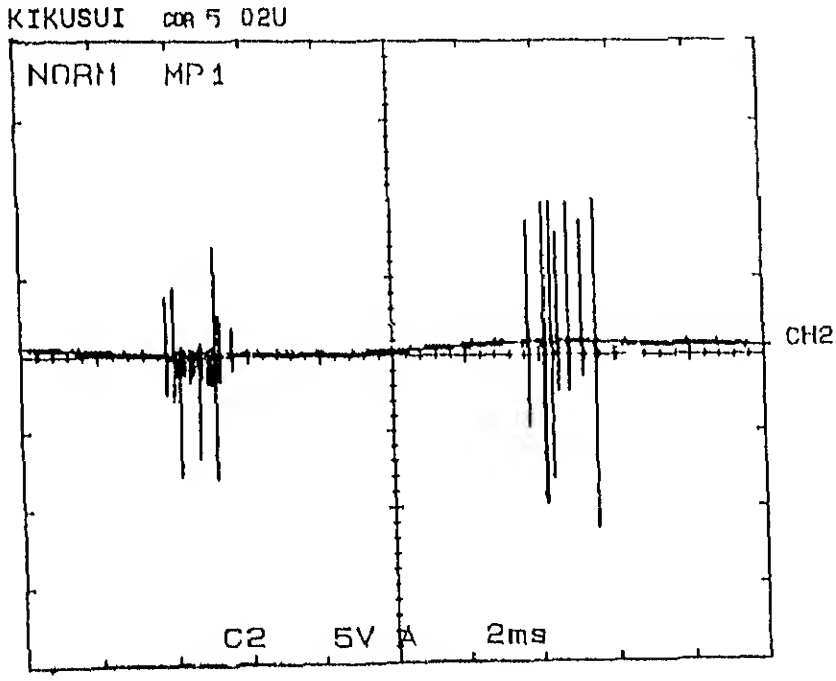

Fig 5 5b The partial discharge pulses after the phase shifter

Fig 5 5 The effect of the phase shifter on the partial discharge measurements

the peak of the triggering sine wave Fig 5 5a 5 5b show the position of the applied voltage before and after using phase shifter respectively

5 2 5 Personal computer

Due to the increasing trend of automatic partial discharge measurement in the recent years the use of digital system has become very popular A personal computer offers the opportunity to store the discharge pulses and to process these in the course of time or a function of power frequency cycle In the present setup Pentium computer having 24 MB RAM 1 6 GB hard disc and 150 MHz speed was used For the pulses of each cycle transferred to personal computer the maximum value of partial discharge pulses has been detected All the pulses which had magnitude of less than 10% of the maximum pulse magnitude in the same half cycle were ignored Therefore generally each pulse has been represented by only its first and second peaks depending upon the relative magnitude of the first peak and subsequent peaks have represented each pulse

5 2 6 Pen Plotter

The MP5300 is a high performance high precision pen plotter that can perform various intelligent functions It is provided with a digital servo system and a 16 bit CPU achieving a maximum plotting speed of 700 mm/second at a mechanical resolution of 0 005 mm For this pen plotter the plotting speed and pen force most suitable for the type of pen being used can be easily selected from the control panel The interface mode is automatically selected when the plotter is connected to a computer or digital

oscilloscope for the respective interface connector When the MP5300 is set to auto RS 232C mode and given data for plotting from the digital oscilloscope the RS 232C settings are automatically selected hence no bother some settings are required This plotter is provided with two types of interfaces for connecting the plotter to a computer or to a digital oscilloscope the centronics compatible parallel interface and the RS232C serial interface

5 2 7 PET 2

The calibrating generator PET 2 was used for the determination of transient response and measuring sensitivity of the partial discharge measuring circuit The circuit is given consideration by a correction factor that can be determined by the supply of defined charge of the calibrating generator into the test circuit

The supply of the natural current from the calibrating generator enables operation of the unit without potential for instance in case of nonearthed test objects Owing to the small dimensions and supply of natural current the calibrating generator PET 2 is of a very low earth capacitance such that the test circuit properties are not being influenced during calibration The unit has been designed for an easy to use construction The photodiode for the generation of the synchronizing pulses are arranged in PET2 Its standard pulse charges output for calibration are 5pC 25pC 50pC 250pC and pulse repetition frequency is 100 Hz and pulse rise time is 50 ns

With the help of PET 2 we have checked our partial discharge detection circuit sensitivity For the calibration we have arranged our circuit as described earlier Fig 5 6 shows the circuit which was used for the

sensitivity calibration In this circuit we have done certain change The coupling capacitor in this circuit is being earthen and PET 2 is connected parallel to the test sample and measuring impedance is also earthen The main criterion in this circuit is that there is no supply voltage is required After completing the circuit when the PET 2 is switched on it starts giving the pulse and detected through digital oscilloscope Our circuit detects minimum pulse charge of 5 pC with the same oscilloscope settings (5 V/cm and 0 2 ms/cm) which was used for the detection of PD pulse This means that our PD detection circuit is able to detect minimum pulse charge of 5 pC

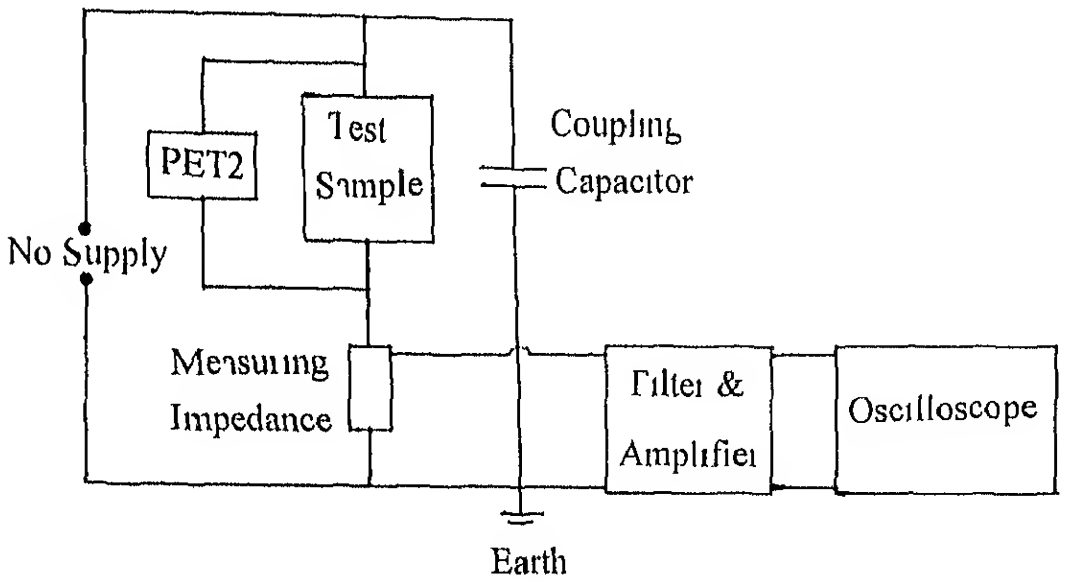

Figure 5 6 Circuit diagram for measuring sensitivity check with PET 2

5 3 Electrode system

A Suitable electrode system which could produce streamer discharge i e avalanche of above critical amplification was needed for investigation of PD Hence for the experiments rod plane electrode system were chosen as

these could produce the desired streamer corona The dimensions of electrode system for investigation in atmospheric air and SF_6 gas were chosen to be the same For the experiments in air a stand of insulating material was used which could hold the electrode system The high voltage was applied to the rod electrode and the plane electrode was earthed Before starting the experiment the electrodes were cleaned by Brasso The dimensions of the electrodes are given in the following section

5 3 1 Glow corona

A point plane electrode system with a gap distance of 10 cm in atmospheric air was used to produced the glow corona The point electrode support was 8 cm long made out of 10mm diameter rod The tip was 12 cm long cone shape with an angle of around 7 The plane electrode having 75mm diameter was given a suitable contour at the brims Partial discharge inception voltage in this case was around 8 kV

5 3 2 Streamer corona

This was produced on rod plane electrode system with increasing gap distance from 1 to 20 cm in atmospheric air The rod electrode chosen had diameters of 8 and 6 mm and lengths of 104mm The tips were given hemispherical shape with radiuses of 7 and 5mm respectively The plane electrode used was of 75mm diameter suitably shaped at the brim The partial discharge inception voltages were measured between 10 to35 kV rms for 6mm rod plane electrode system and 11 to 47 kV rms for 8mm rod plane electrode systems for gap distances between 1 to 20 cm

5.3.3 SF_6 glass vessel

For the measurement of PDIV in SF_6 gas two glass vessels were fabricated Their lengths were 235mm and diameter 100mm For high voltage electrode 6 and 8mm polished rod and for ground electrode plane of 70mm diameter having curved brim were chosen Both the HV and the ground electrodes were fixed inside the vessel after sealing the vessel with help of quick fix At one end of the glass tube plane electrode was fixed Other end of the glass tube was fitted with a hollow metal electrode The rod electrode was placed inside the hollow metal tube with a high pressure O ring sealing metal washer and a nut The O ring was provided in order to vary the gap distance and a washer helped to fix the O ring with the electrode Figure 5.7a shows the variable gap distance arrangement Near the high voltage electrode another hollow metal tube was placed A pressure gauge and a pressure valve were attached with this tube by brazing The total attachment was fixed with the glass tube Figure 5.7b shows the variable pressure arrangement and figure 5.8 shows the overall arrangement of the system Before fixing the electrode system within the glass vessel the electrodes were cleaned with Brasso After fixing the variable electrode system and the variable pressure arrangement the total vessel was attached with the vacuum pump for creating vacuum When the vacuum reached to about 10^{-5} Torr then the SF_6 gas filling was started with precaution Initially the gas was filled upto a pressure of 0.2 MPa with the help of regulator The regulator had two gauges one of them measured cylinder pressure and the other measured vessel pressure An extra gauge which was placed before the pressure valve showed also the vessel pressure With the help of pressure

valve variable pressure filling could be achieved by slowly releasing the gas

5.4 Conclusion

In this chapter the partial discharge measuring circuit as well as the different electrode system used to generate the partial discharge have been described These PD sources produced glow corona streamer corona The point plane electrode system produced glow corona and rod plane electrode system produced streamer corona

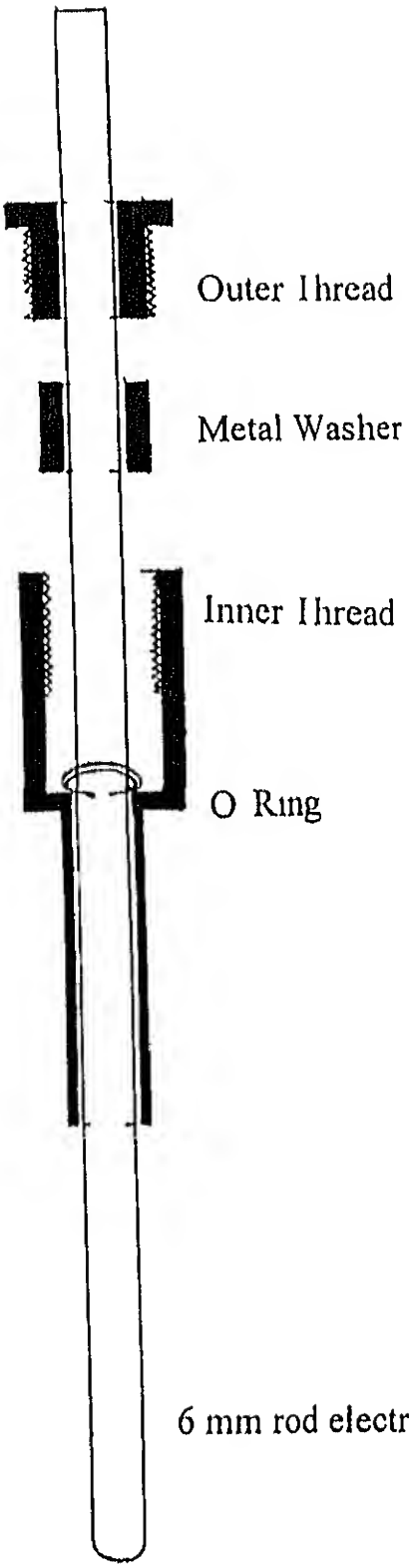

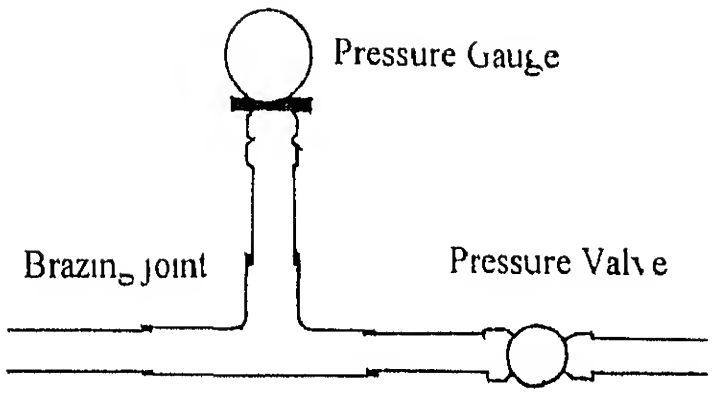

Figure 5.7b Variable pressure arrangement

Figure 5.7a Variable gap distance arrangement

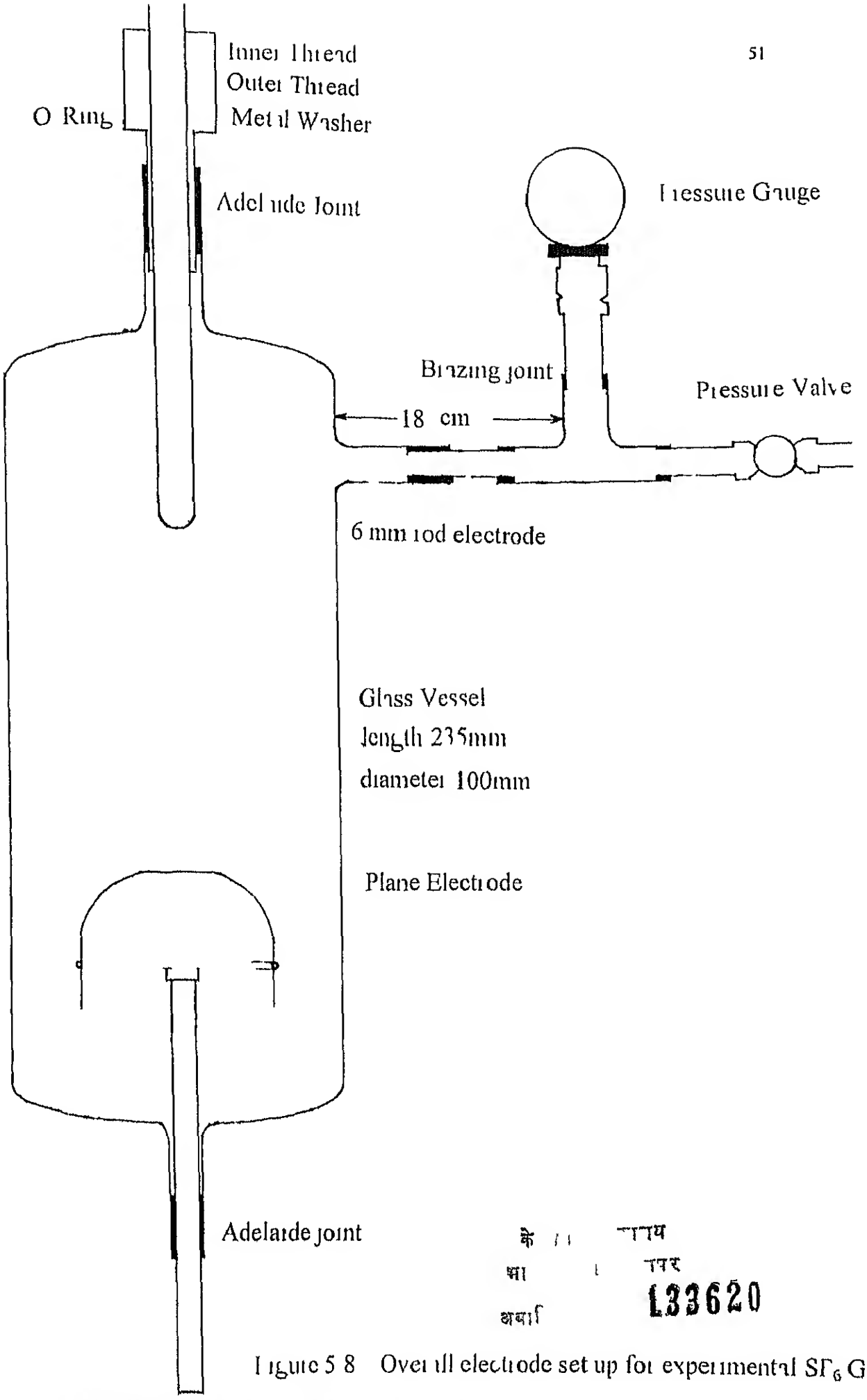

Figure 5 8 Overall electrode set up for experimental SF_6 G

Chapter 6

Experimental Investigation and test results

In this chapter the laboratory investigations performed and the test results obtained are discussed

6 1 Inspection of the measuring circuit for I D

In order to ensure that the measuring circuit is free of PD up to the highest voltage of investigation in these experiments the circuit shown in fig 5 1 was checked without the test sample and H V High voltage was applied to determine if any partial discharge in the measuring circuit occurred In this case taking the gap distance between the electrode on which the test object electrode was fixed and earth to be more than 15cm the measuring circuit was checked increasing the supply voltage upto 65 kV for the occurrence of any PD It was observed that no partial discharge occurred Hence it could be concluded that the measuring circuit and the power supply used for the measurement of partial discharge was PD free upto 65 kV This was necessary to ensure that the measured PD occurred only at the desired test object

6 2 1 Measurement of PD inception level in air with needle plane electrode

The measurements were performed with a cone shaped brass needle electrode of length 10cm having a diameter of the tip to be 1mm and the

cone angle of 7 An inverted bowl shaped plane electrode of diameter 70mm was chosen Maintaining a gap distance between the needle and plane electrodes to be 10cm and using the circuit given in figure 5 1 the PD measurement were made with increasing voltage At about 8 kV the first partial discharge pulses were observed by the oscilloscope Figure 6 1 shows the I D pulses measured on needle plane electrode configuration drawn by the plotter MP5300 after interfacing with oscilloscope

6 2 2 Measurement of I D inception level in air with 8mm rod plane electrode

This experiment was conducted with rod and plane electrode system The dimension of the plane electrode was same as before The diameter of the rod was 8mm its length was 104mm and the tip was hemispherical having a radius of 7mm Using the same circuit with this electrode system the first partial discharge pulses were observed at 27 5 kV for a 10 cm gap distance Figure 6 1 shows the partial discharge inception pulses detected on the oscilloscope and plotted by the plotter

6 2 3 Measurement of PD inception level in air with 6mm rod plane electrode

With the same circuit and same plane electrode this experiment was conducted but the dimensions of the rod electrode were different The diameter of the rod electrode was 6mm length 120mm and the tip was hemispherical shaped with a radius of 5mm The first partial discharge inception pulses in this case could be measured at 25 kV Figure 6 1 shows

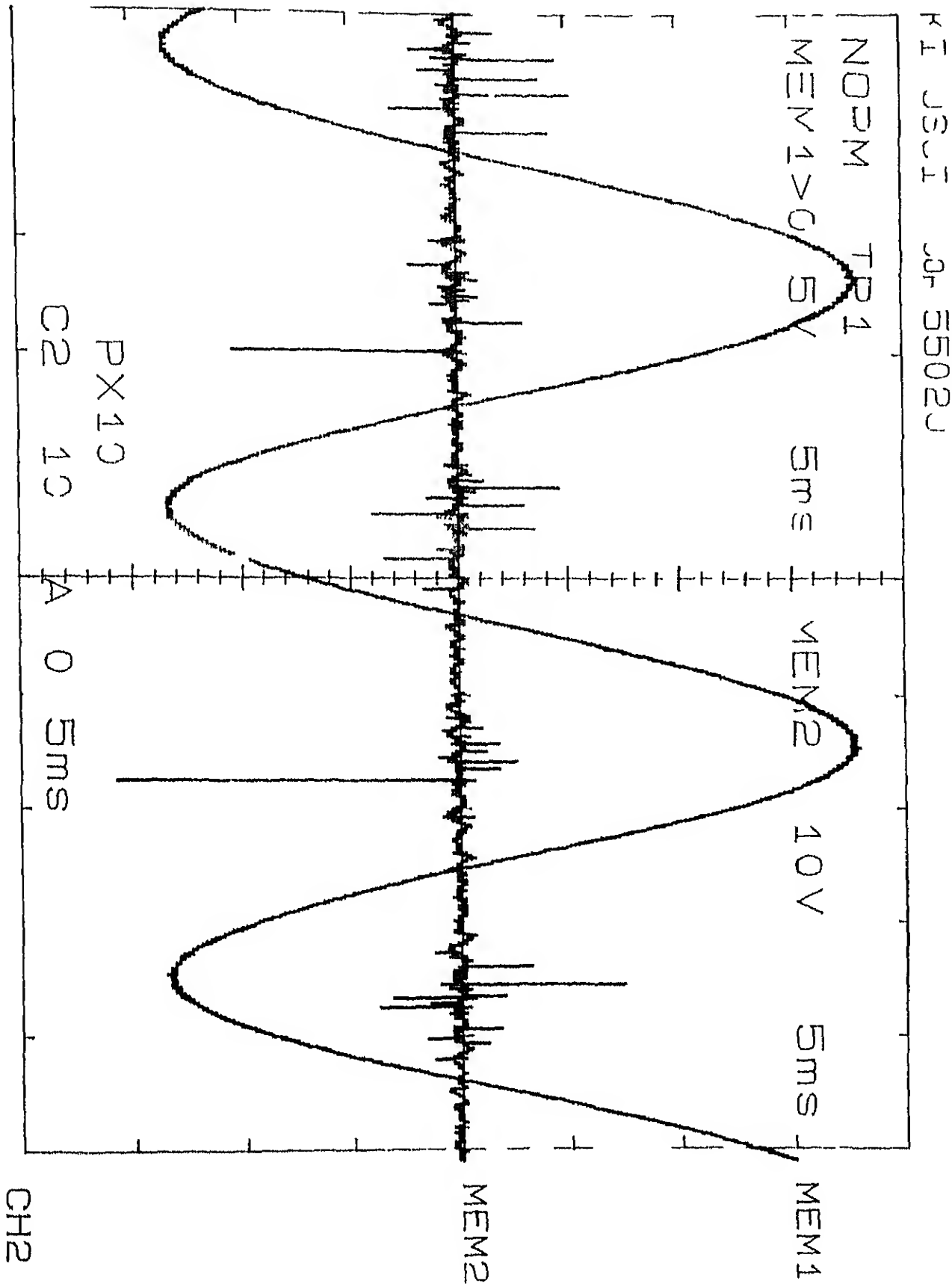

Figure 6 1 Partial Discharge pulse detected through oscilloscope

the partial discharge pulses measured on 6mm rod plane electrode configuration

6.3 Experiments with increasing gap distance in air for audible measurable PDIV and BDV

With the same circuit described before these experiments were performed with two electrode systems 6 and 8mm rod and plane electrodes For these experiments were performed at gap distance between 1and 20 cm The increasing gap distance set were 1 2 3 4 5 7 10 11 12 13 15 18 and 20cm First the breakdown voltages and audible P D inception voltages with increasing gap distance were measured The audible PD inception was heard with naked ears by the observer at a distance of about 3m (behind the lab fence) Both these readings were taken one after the other shown in Table 6 1 Figure 6 2 and 6 3 show the curves between Audible PD inception and breakdown voltages with increasing gap distance for 6 and 8mm rod plane electrode systems respectively It can be observed that the breakdown and PD inception voltages have a very negligible difference initially for the gap distances of 1 & 2cms which has an increasing trend with increasing gap distances Above 12 cm gap distance the breakdown voltage increases to double the magnitude of PD inception voltage and continues to show a rising characteristics Audible PDIV shows a flat characteristics with increasing gap distance From these characteristics an idea about magnitudes of PD inception and breakdown voltages is obtained It can be observed that the voltage differences which are negligible initially are quite small for small gap distances but above a gap distance of 12cm it is almost double and at 20cm it becomes even 2 5 times

Figure 6.4 shows the measurable PD inception and breakdown voltages characteristics with increasing gap distance. The measured PDIV was detected with the help of PD measuring circuit on the digital oscilloscope. The curves on this figure show that the measured PDIV has a flat characteristic for both the electrode systems and the 6mm rod has a lower PDIV than for the 8mm rod. Breakdown voltage characteristic has an increasing trend and in this case also lower breakdown voltages are measured in case of 6mm rod than for 8mm rod. This means the sharper is the electrode lower is the Schwaiger factor (η) and hence lower is the breakdown strength of the gas. PDIV voltages are always lower than that of breakdown voltages and difference between them increases tremendously beyond the gap distance of 12cm. These curves provide an idea about the voltage level difference of the two phenomena i.e. the PDIV (U) and breakdown (U_b) for the electrode systems used in our experimental investigations.

Figure 6.5 shows the characteristics curves between audible PD and measurable PD inception voltages with increasing gap distances for 6 and 8mm rod plane electrode systems brought together. From these curves it can be observed that PD inception voltage for 6mm rod is lower than that for 8mm rod in the both the cases and also that measured PDI voltage is lower than the audible PDIV in both the cases. Once again it reveals that the PDIV depends upon the sharpness of the electrode hence upon the Schwaiger factor. The measured PDIV characteristics for longer gap distance is flatter. The measured PDIV with measuring circuit was detected by the digital oscilloscope and the audible PD was heard by ears through the flutter sound produced by the corona activity. The sensitivity of the measuring circuit

described in section 5 2 7 was 5pC whereas the sensitivity of the audible corona was the observers ears

Gap distance In cm	Breakdown voltage U_b in kV (peak) rms $\times\sqrt{2}$	Partial discharge inception voltage PPIV (audible) U in kV (peak) rms $\times\sqrt{2}$
1 cm	16 92	15 56
2 cm	22 62	21 21
3 cm	28 28	24 04
4 cm	35 35	28 28
5 cm	41 01	31 11
7cm	46 66	33 94
10 cm	60 01	39 59
11 cm	66 46	41 01
12 cm	73 53	43 84
13 cm	86 1	45 25
15 cm	98 98	46 66
18 cm	113 12	48 06
20 cm	130 10	49 49

Table 6 1 Audible PDIV and BDV with variable gap distance for 6mm rod plane electrode system in air

Gap distance in cm	Breakdown voltage U_b in kV (peak) rms×√2	Partial discharge inception voltage PDIV (audible)U in kV (peak) rms×√2
1	19 74	16 26
2	25 45	22 62
3	32 52	26 87
4	38 18	32 52
5	43 84	38 18
7	53 74	42 42
10	63 63	50 91
11	69 29	55 15
12	77 78	56 59
13	96 16	59 59
15	113 13	62 22
18	120 20	63 63
20	132 93	66 46

Table 6 2 Audible PDIV and BDV with variable gap distance for 8 mm rod plane electrode system in air

Gap distance in cm	Audible PDIV for 8mm rod kV (peak) rms×√2	Audible PDIV for 6mm rod kV (peak) rms×√2	Measured PDIV for 8mm rod kV (peak) rms×√2	Measured PDIV for 6mm rod kV (peak) rms×√2
1	16 26	15 51	14 1	12 26
2	22 62	21 21	18 38	16 97
3	26 87	24 04	21 21	19 79
4	32 52	28 28	26 86	25 45
5	38 18	32 52	31 11	28 28
10	50 91	41 01	38 89	35 35
12	56 59	43 94	39 59	36 76
15	62 22	46 66	40 3	38 89
20	66 46	49 49	41 71	40 3

Table 6 4 Measured PDIV and Audible PDIV with increasing gap distance for 8 and 6mm rod plane electrode system in air

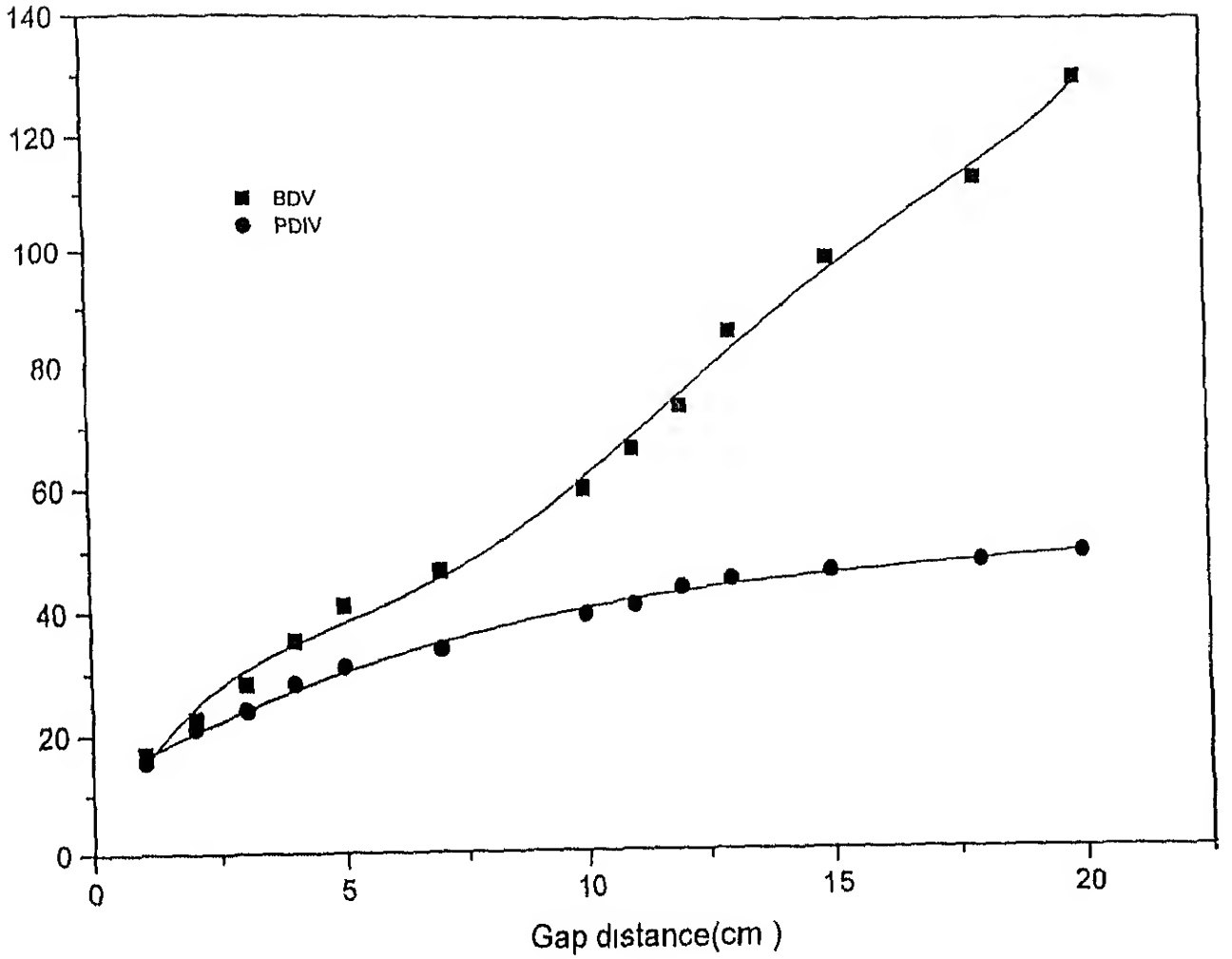

Figure 6.2 Audible PDIV and BDV characteristics with increasing gap distance in air for 6mm rod plane electrode system

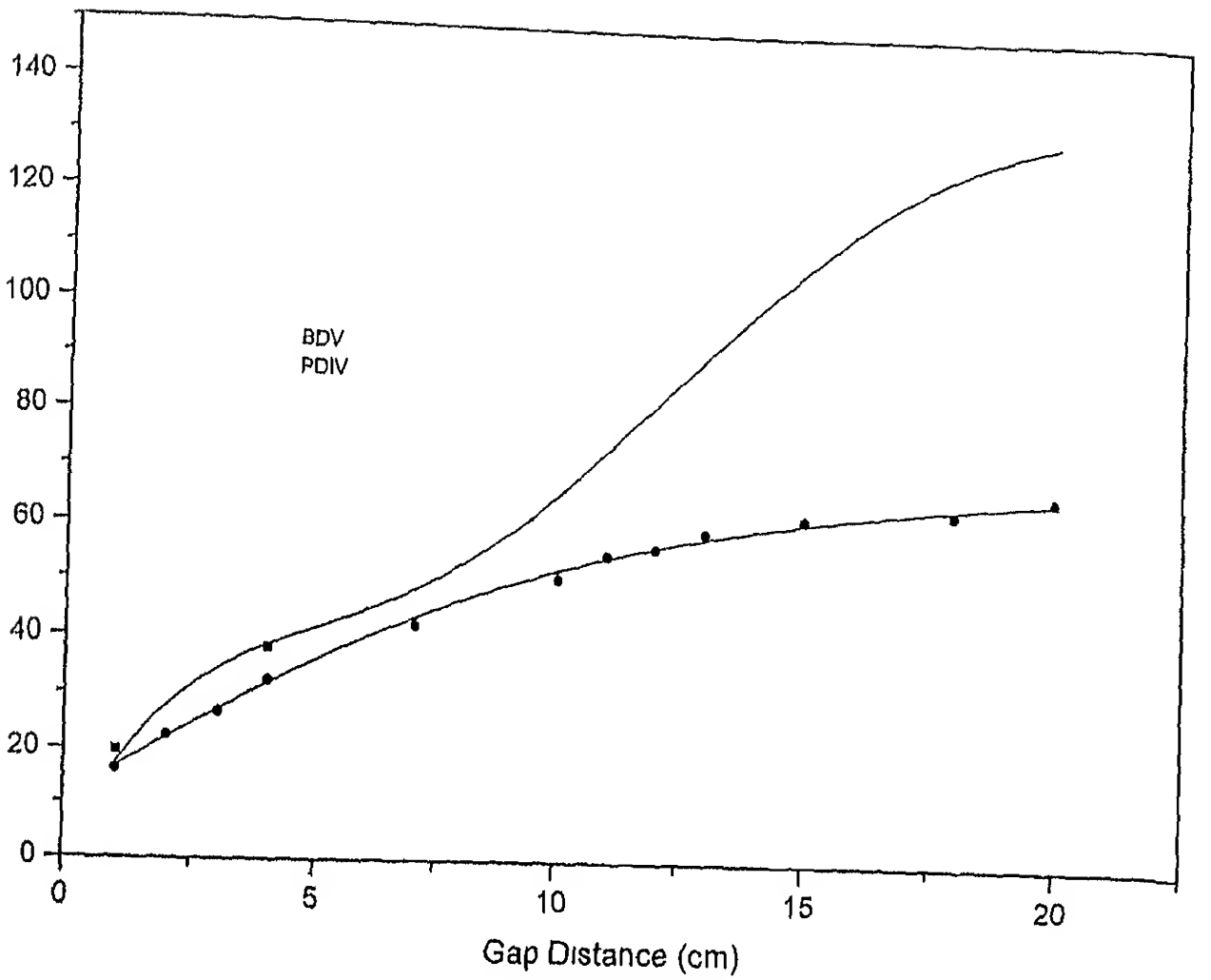

Figure 6.3 Audible PDIV and BDV characteristics with increasing gap distance in air for 8mm rod plane electrode system

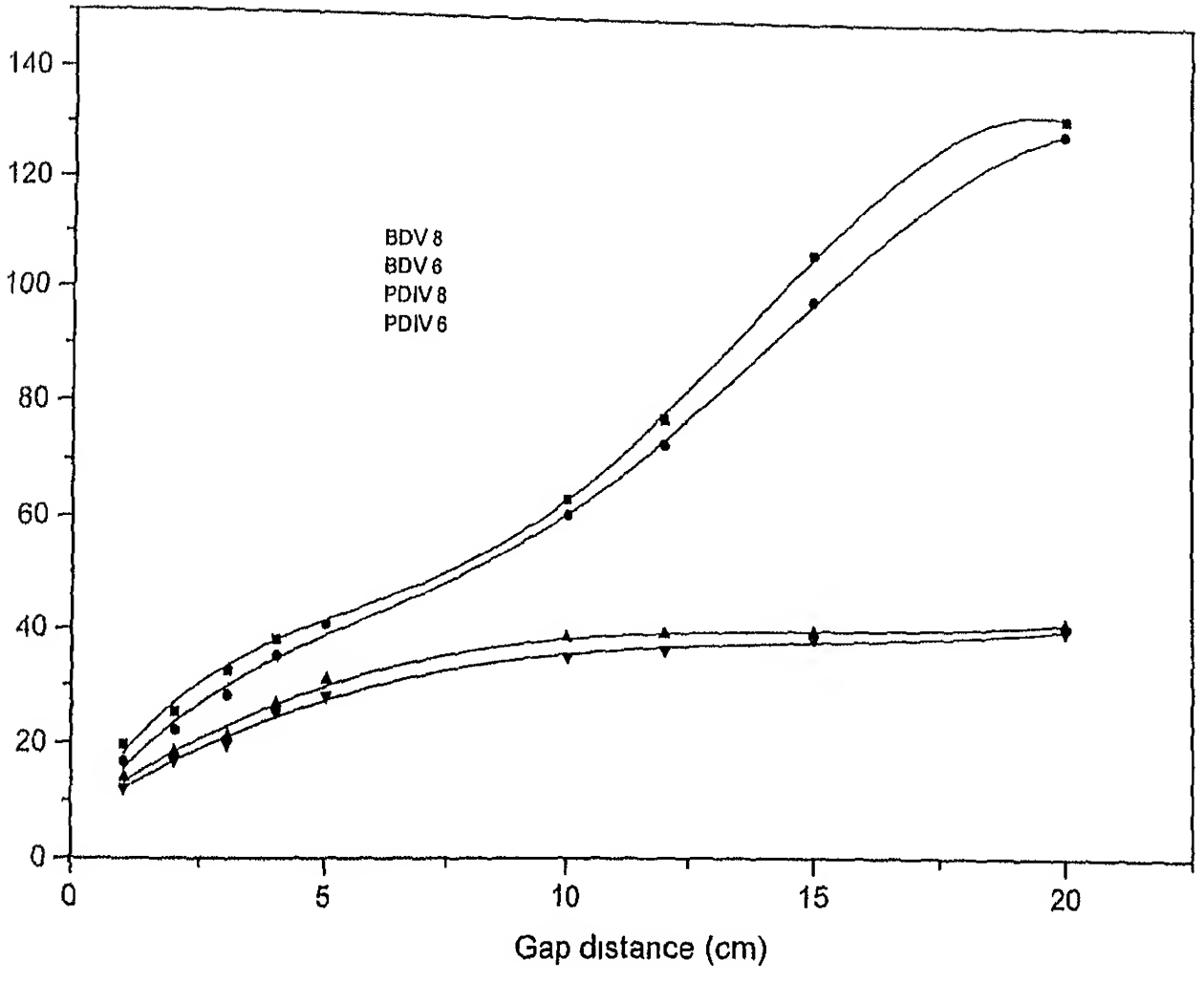

Figure 6.4 Measured PDIV and BDV characteristics with increasing gap distance in air for 6 & 8mm rod plane electrode system

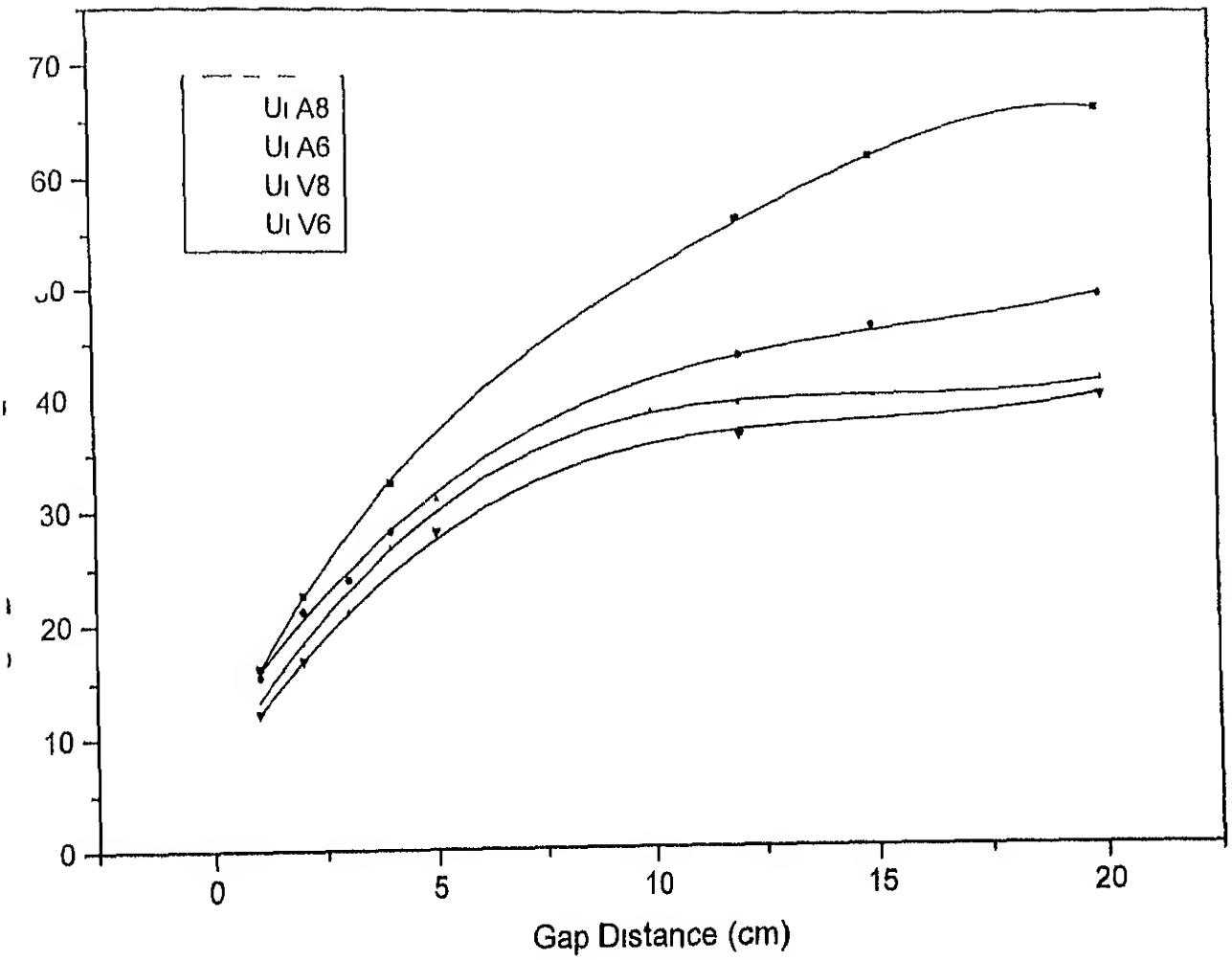

Figure 6.5 Measured and audible PDIV characteristics with increasing gap distance in air for 6 & 8mm rod plane electrode system

6.4 Experiment in SF_6 Gas

Using the same circuit as shown in fig 5.1 the PDIV measurements were performed in SF_6 gas. The electrode system chosen was 6mm rod plane considering its property of lower PDIV. For these experiments the gap distances of 1, 2, 3 upto 15cm could be set with help of a variable gap distance setting arrangement. Experiments could also be performed at different pressures with help of a variable pressure arrangement in the vessel. only partial discharge inception voltages were measured in SF_6 gas. The breakdown voltages were not measured in order to prevent decomposition of gas affecting the PDIV. The pressures at which PDIV measured at different gap distance settings were 3, 2.5, 2.0, 1.5 and 1.0atm. Figure 6.6 shows the characteristics curve between partial discharge inception voltage vs gap distance at different constant gas pressures. All the curves show almost a flat characteristics above a gap distance of around 6cm. It can be observed that as the gas pressure is increased the PDIV also increase. It can be concluded that PDIV is a function of gas pressure. PDIV increases with increasing gap distances initially for relatively shorter gap distances and then no significant increase is measured for gap distances above 6cm upto a gas pressure of 2 atm. Above this pressure the flat characteristics of the curve is measured above slightly longer gap distance. When pressure was high i.e. 3 atm pressure it was observed beyond 9cm gap distance and when the pressure was low it was observed above 6cm gap distance at 1 atm pressure. It can also be observed that upto a gas pressure of 2.5 atm the readings of all PDIV are not much different however at 3 atm pressure the difference measured is significant. At the gap distance of 15cm

PDIV measured was 29 kV (rms) at 1atm pressure but at the same gap distance 43 kV (rms) was measured at 3 atm pressure

Fig 6 7 shows the relation between PDIV and gas pressure at constant gap distances Three different gap distances of 1 5 and 10cm have been chosen for plotting these characteristics Curve 1 is the characteristics of 1cm gap curve 2 and curve 3 for 5 and 10 cm gap distances respectively Above 10cm gap distance no significant difference in PDIV are measured on increasing the gap distance at all the pressures However the PDIV increases with the increasing pressure

6 5 Comparison between the measurements in SF_6 and air

Comparing the measured results of PDIV in atmospheric air and SF_6 following can be observed

1 At 1 atm pressure PDIV are measured to be at higher voltages in SF_6 than in air for the same 6mm rod plane electrode system
2 The difference in PDIV has been measured to be very high for small gap distances upto the order of 5cm which reduces considerably on increasing the gap distance further At and around 15 cm gap distance the difference has been measured to be marginal as seen from the fig 6 8
3 When the pressure increases then the partial discharge inception voltages also increases At 1 atm pressure PDIV in air for 6mm rod plane electrode system at the gap distance of 10 cm was measured to be 25 kV rms but for the same gap distance and same electrode system in SF_6 gas it was 29 kV rms which increased to 43 kV rms at 3 atm pressure

Gap distance In cm	PDIV kV (peak) rms×√2 at 3 0 Atm pressure	PDIV kV (peak) rms×√2 at 2 5 Atm pressure	PDIV kV (peak) rms×√2 at 2 0 Atm pressure	PDIV kV (peak) rms×√2 at 1 5 Atm pressure	PDIV kV (Peak) rms×√2 at1 0 Atm pressure
1	41 01	36 76	35 25	33 94	32 52
2	47 37	39 59	38 18	36 76	35 35
3	49 49	41 01	39 59	38 18	36 76
4	52 35	42 42	41 01	39 59	38 18
5	53 74	43 84	42 42	41 01	39 59
6	55 15	45 25	43 84	42 42	40 30
7	56 56	46 66	44 54	43 13	41 01
8	59 39	48 08	45 25	43 13	41 01
9	60 81	49 49	45 96	43 13	41 01
10	60 81	49 49	45 96	43 13	41 01
11	60 81	49 49	45 96	43 13	41 01
12	60 81	49 49	45 96	43 13	41 01
13	60 81	49 49	45 96	43 13	41 01
14	60 81	49 49	45 96	43 13	41 01
15	60 81	49 49	45 96	43 13	41 01

Table 6 5 Partial Discharge inception Voltage and variable gas pressure with increasing gap distance in SF_6 gas

Gas pressure (Atmospheric)	PDIV kV (peak) rms×√2 at1 0 cm gap distance	PDIV kV (peak) rms×√2 at 5 0 cm gap distance	PDIV kV (peak) rms×√2 at10 0 cm gap distance
1 0	32 52	39 49	41 01
1 5	33 94	41 01	43 13
2 0	35 35	42 42	45 96
2 5	36 76	43 84	49 49
3 0	41 01	53 74	60 81

Table 6 6 Partial discharge inception voltage and gap distance with increasing gas pressure in SF_6 gas

Gap Distance in cm	PDIV for SF_6 gas in kv (peak) rms×√2 at atm Pressure	PDIV for air in kV (peak) rms×√2 at atm pressure
1	32 52	12 26
2	35 35	16 97
3	36 76	19 79
4	38 18	25 45
5	39 59	28 28
10	40 01	35 35
12	40 01	36 76
15	40 01	38 89

Table 6 7 Measured PDIV with increasing gap distance in air and SF_6 gas for 6mm rod plane electrode system at 1 atm pressure

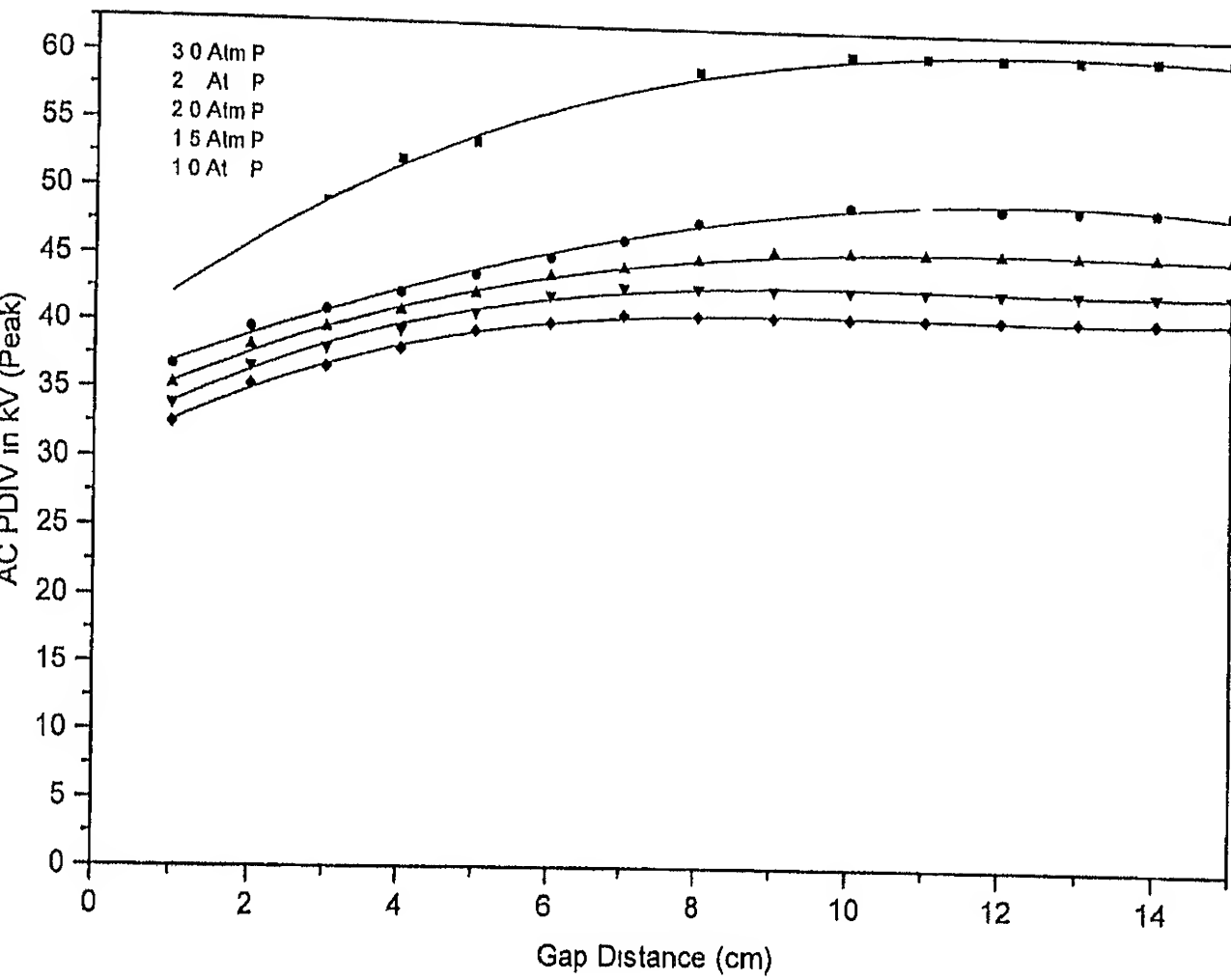

Fig 6 6 Measured PDIV Characteristics with increasing gap distance at constant pressure in SF_6 gas for 6mm rod plane electrode

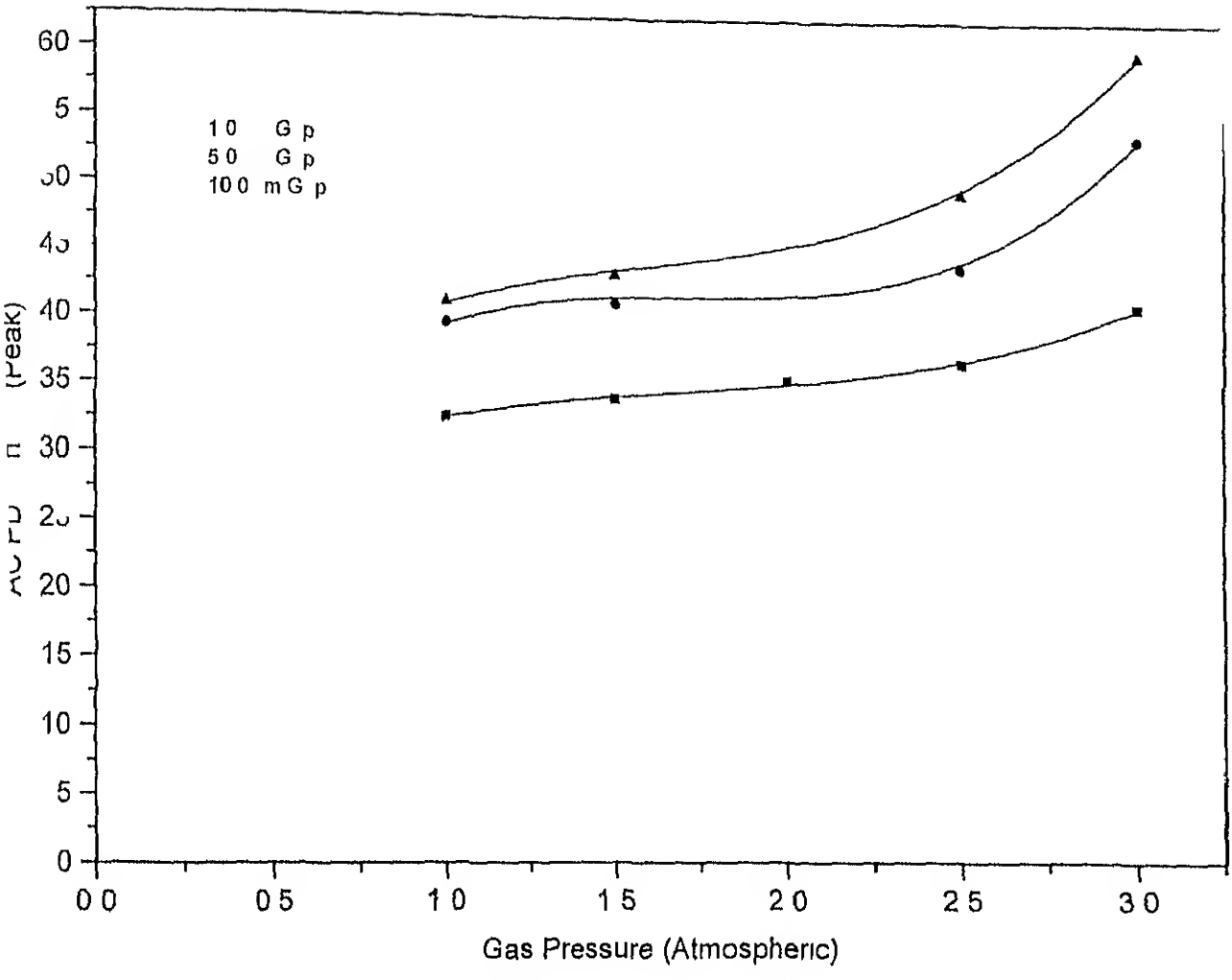

Fig 6 7 Measured PDIV characteristics with increasing gas pressure at constant gap distance in SF_6 gas for 6mm rod plan electrode

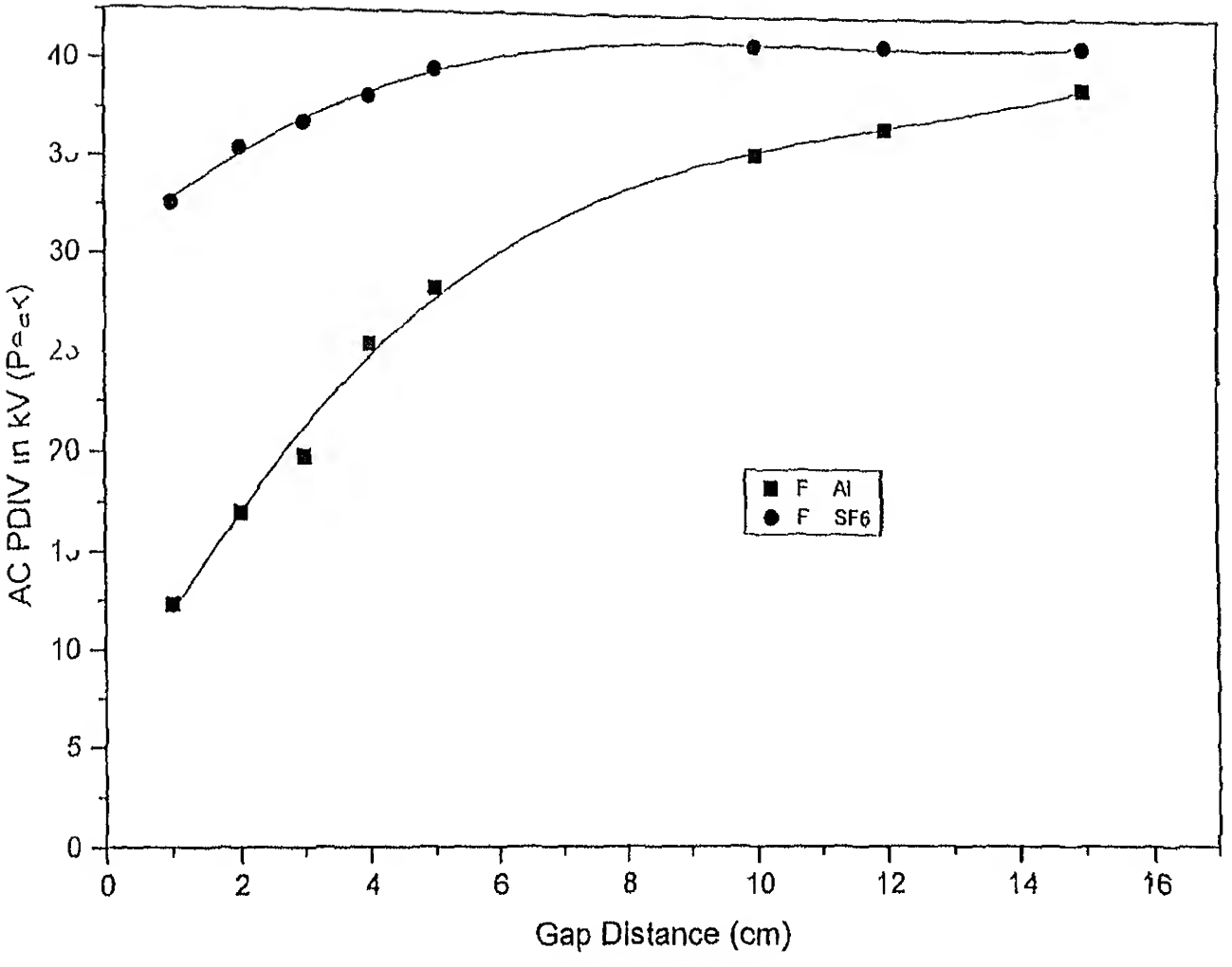

Fig 6 8 PDIV characteristics with increasing gap distance in air and SF_6 gas for 6mm rod plane electrode system at atmospheric pressure

Chapter 7

Conclusions and Scope of Future Work

7.1 Results And Conclusions

Partial Discharge is an electric discharge that does not bridge the insulation It gives rise to electric pulse current of magnitudes depending upon the applied voltage and the pulse position with respect to voltage waveform It has been recognized that the breakdown of insulation of electrical equipment often occurred by the occurrence of partial discharge within or on the surface of the insulation Therefore if the partial discharge is found to take place in any insulation system it is important to identify its source In other words there is a necessity to identify and classify the unknown partial discharge source In this work partial discharge inception voltages are measured in air and SF_6 gas The experiments have been conducted with 8 and 6mm rod as high voltage and plane electrode as ground at varying gap distance The measurements in air were also conducted with needle plane electrode system at atmospheric pressure In SF_6 gas the experiments were performed only with 6 mm rod plane electrode system at different pressures upto 3 atm Pressure With the rod plane electrode system since the fall of electric field intensity at the tip of rod is not so steep it can be assumed that the PD takes place with above critical amplification of avalanche which gives rise to streamer corona On the contrary at the needle tip PD takes place with bellow critical amplification of avalanche

In case of experiments conducted in air following conclusions can be drawn from the measured results

1 With the needle plane electrode system PDIV observed were at lower voltage than that for rod plane electrode system because of its sharpness At any sharp edge electrode partial discharge incept at lower voltages

2 As the breakdown voltages measured are greater than the PDIV it can be concluded that stable partial discharges precede the breakdown

3 Breakdown voltages have a rising characteristics whereas partial discharge characteristics above a gap distance are flat with respect to increasing gsp distances

4 In case of rod plane electrode when the rod diameter is increased i e the tip area increases or the field becomes less nonuniform PDIV also increases It can be concluded that PDIV is a function of the degree of uniformity (η) the Schwaiger factor

5 The magnitude of the audible PDIV which was detected through flutter sound heard by the human ears is higher than the measured PDIV This concludes that any corona that we hear with ear is an advance stage of corona or partial discharge

For the experiments conducted in SF_6 gas the following conclusions can be drawn

1 Partial discharge inception voltage is higher in SF_6 gas than that for air at normal atmospheric pressure for the same electrode configuration and gap distance This difference in PDIV has been measured to be very high for small gap distances For 6mm diameter rod plane electrode the difference in PDIV at 1cm gap is measured to be more than 2 5 times (12 26 & 32 52 kV) and for 5cm gap it reduces to 1 4 times At and around 15 cm gap distance the difference has been measured to be marginal of the order of only one kV It can be concluded here that when the field is more uniform (small gap distance) the difference in PDIV

between air and SF_6 is large whereas it is marginal when the field becomes more nonuniform (long gap distance)

2 As the pressure is increased the magnitude of PDIV in SF_6 gas also increases however upto the pressure of 2 5 atm this increase is not too significant It can be concluded that the PDIV at rod electrode is a function of the gas pressure in the gap

3 At 3 atm and higher pressure the PDIV increases significantly higher than at 2 5 atm pressure

4 Like in air in SF_6 gas also the PDIV characteristics were flat above a certain gap distance at all the pressures of the measurement

7 2 **Scope of future works**

The present work in SF_6 gas is only for variable gap distance and variable pressure for 6 mm electrode only It can be repeated with variable diameter of rod electrodes and also for needle plane electrode system This work is also valid only for non uniform field It can also be done in uniform and weakly non uniform fields by changing the electrode systems

2 In the present work it has possible to carry out investigations upto 3 0 atmospheric pressure in SF_6 gas due to constraints of time and glass vessel It should be preferred at more than 3 0 atm preferably upto 5 atm pressure in SF_6 gas in another suitable experimental vessel

3 In present work investigations have been performed with alternating power frequency voltage It would be worth continuing similar investigations with lightning and switching impulse voltages of different wave shapes However this will require more elaborate development of the experimental vessel

between air and SF_6 is large whereas it is marginal when the field becomes more nonuniform (long gap distance)

2 As the pressure is increased the magnitude of PDIV in SF_6 gas also increases however upto the pressure of 2 5 atm this increase is not too significant It can be concluded that the PDIV at rod electrode is a function of the gas pressure in the gap

3 At 3 atm and higher pressure the PDIV increases significantly higher than at 2 5 atm pressure

4 Like in air in SF_6 gas also the PDIV characteristics were flat above a certain gap distance at all the pressures of the measurement

7 2 **Scope of future works**

The present work in SF_6 gas is only for variable gap distance and variable pressure for 6 mm electrode only It can be repeated with variable diameter of rod electrodes and also for needle plane electrode system This work is also valid only for non uniform field It can also be done in uniform and weakly non uniform fields by changing the electrode systems

2 In the present work it has possible to carry out investigations upto 3 0 atmospheric pressure in SF_6 gas due to constraints of time and glass vessel It should be preferred at more than 3 0 atm preferably upto 5 atm pressure in SF_6 gas in another suitable experimental vessel

3 In present work investigations have been performed with alternating power frequency voltage It would be worth continuing similar investigations with lightning and switching impulse voltages of different wave shapes However this will require more elaborate development of the experimental vessel

Reference

1 Alston R and Mosch W High voltage Insulation Engineering And Behavior Of Dielectrics Wiley Eastern Limited 1995

2 Herve Champion[1] Alice Goldman Micail Lamas[2] From Corona Stabilization To Spark Breakdown In Point To Plane SF_6 Gas Gaseous Dielectrics VIII 1998 pp 113

3 Yamada[1] T Takahasi[1] T Toda[2] T and Okubo[1] H Generation Mechanism Of Partial Discharge In Different Kind Of Pure Gases And Gas Mixtures With SF_6 Gaseous Dielectrics VIII 1998 New York pp 125

4 Yamada[1] T Takahasi[1] T Okubo[1] H and Hitika M Dependence Of Partial Discharge And Breakdown Characteristics On Applied Power Frequency In SF_6 Gas Gaseous Dielectrics VIII 1998 New York pp 295

5 Goffar Khan M A Investigation Of Insulating Properties Of Vacuum Under High Voltage Ph D Thesis Dept Of Electrical Engg I I T Kanpur 1995

6 Yamada[1] F Takahasi[1] T Toda[2] T and Okubo[1] H Partial Discharge Inception And Breakdown Characteristics In Gas Mixtures And SF_6 Gaseous Dielectrics VIII 1998 New York pp 289

7 Morrison H D Chu F Y Braun J M Ford G L A Utility Perspective On SF_6 Gas Management Issues Gaseous Dielectrics VIII 1998 New York pp 557

8 Mohamed Kamal ABD EL Rahaman Classification of Partial Discharge Patterns Using Texture Analysis Algorithms Ph D Thesis Dept of Elect Engg I I T Kanpur June 1999

9 Captain Sunil Prem An Investigation Of Schwaiger Factor Limit in Air M Tech Thesis Dept Of Elect Engg I I T Kanpur April 1994

10 Eric Ray Dolin[1] The United States Environmental Protection Agencys SF_6 Emissions Reduction Partnership For Electric Power System An Opportunity For Industry Gaseous Dielectrics VIII 1998 New York pp 425

11 Pedersen A On The Electrical Breakdown Of Gaseous Dielectric An Engineering Approach IEEE Transaction On Electrical Insulation Vol 24 No 5 Oct 1989 PP 721

12 H R Goxiola Wetzer M Joseph A Study Of Prebreakdown in SF_6 Gaseous Dielectrics VIII 1998 New York pp 105

13 Yamada[1] T Takahasi[1] T Okubo[1] H and Hitika M Discrimination Of Streamer/Leader Type Partial Discharge In in SF_6 Based On Discharge Mechanism Gaseous Dielectrics VIII 1998 New York pp 269

14 Fuhr J Hussing M Konigstein D Fiorkowski M PD System On Site Detection Of Aging Processes In High Voltage Apparatus 7th International Sysposium On High Voltage Engineering August 28 30 1991 Diesden pp 93

15 A Schettler D Peier A New Computer Aided Partial Discharge(PD) Mersuring System For Dielectric Dignosis 7thInternationalSysposiumOn High Voltage Engineering August 28 30 1991 Diesden pp 101

133620

Date Slip

The book is to be returned on the date last stamped